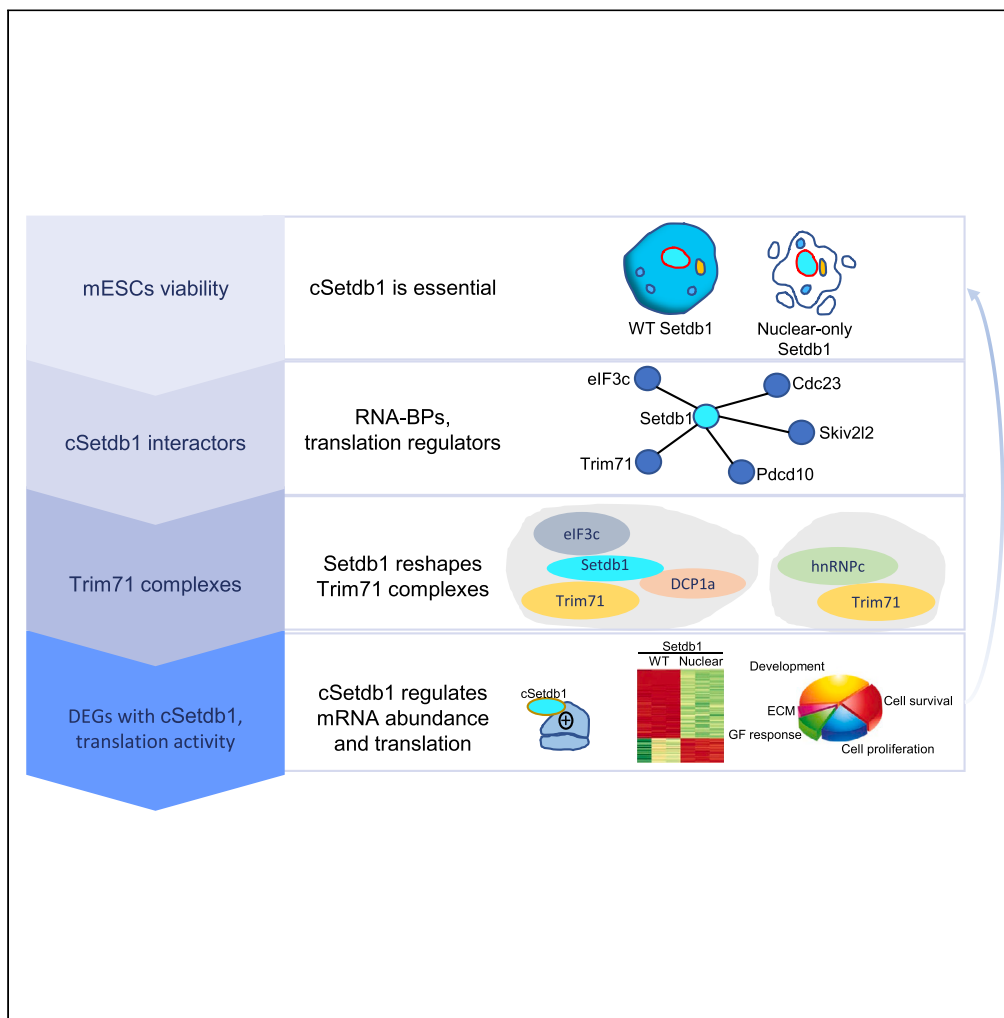**Article**

The cytoplasmic fraction of the histone lysine methyltransferase Setdb1 is essential for embryonic stem cells

Roberta Rapone, Laurence Del Maestro, Costas Bouyioukos, ..., Véronique Joliot, Bertrand Cosson, Slimane Ait-Si-Ali

bertrand.cosson@u-paris.fr (B.C.)
slimane.aitsiali@u-paris.fr (S.A.-S.-A.)

Highlights

Cytoplasmic Setdb1 (cSetdb1) is required for mES cells survival

Setdb1 interacts with many RNA-BPs and translation regulators such as Trim71

Setdb1 is required for Trim71 complex integrity

cSetdb1 regulates the abundance of specific mRNAs, of which Trim71 and hnRNPc targets

Article

The cytoplasmic fraction of the histone lysine methyltransferase Setdb1 is essential for embryonic stem cells

Roberta Rapone,[1] Laurence Del Maestro,[1] Costas Bouyioukos,[1] Sonia Albini,[1] Paola Cruz-Tapias,[1] Véronique Joliot,[1] Bertrand Cosson,[1,2,*] and Slimane Ait-Si-Ali[1,2,3,*]

SUMMARY

The major lysine methyltransferase (KMT) Setdb1 is essential for self-renewal and viability of mouse embryonic stem cells (mESCs). Setdb1 was primarily known to methylate the lysine 9 of histone 3 (H3K9) in the nucleus, where it regulates chromatin functions. However, Setdb1 is also massively localized in the cytoplasm, including in mESCs, where its role remains elusive. Here, we show that the cytoplasmic Setdb1 (cSetdb1) is essential for the survival of mESCs. Yeast two-hybrid analysis revealed that cSetdb1 interacts with several regulators of mRNA stability and protein translation machinery, such as the ESCs-specific E3 ubiquitin ligase and mRNA silencer Trim71/Lin41. We found that cSetdb1 is required for the integrity of Trim71 complex(es) involved in mRNA metabolism and translation. cSetdb1 modulates the abundance of mRNAs and the rate of newly synthesized proteins. Altogether, our data uncovered the cytoplasmic post-transcriptional regulation of gene expression mediated by a key epigenetic regulator.

INTRODUCTION

Embryonic stem cells (ESCs) fate is influenced by transcriptional and post-transcriptional regulation of gene expression. The role of transcription factor regulatory networks in combination with chromatin modifying proteins in ESCs fate have been extensively studied. Increasing evidence shows that mRNA stability and mRNA translation are also finely tuned and strongly control the pluripotency and the fate of ESCs.[1] Moreover, an increasing number of RNA-binding proteins (RBPs) involved in post-transcriptional and translational regulation of gene expression have been identified and described as regulatory of ESC identity.[2–4]

Setdb1 (also called ESET/KMT1E) is a histone 3 lysine 9 (H3K9) lysine methyltransferase (KMT) which belongs to the SUV39 family, and a major epigenetic regulator of transcriptional gene repression. *Setdb1* knockout (KO) is lethal in mice at the peri-implantation stage.[5] Setdb1 is essential for the survival of mESCs and it influences ESCs identity, pluripotency, and self-renewal.[6–8] Setdb1 is also required for the cell survival, pluripotency maintenance, and terminal differentiation of many progenitor cell types. Setdb1 is necessary for the survival of spermatogonial progenitors in mice[9] and a mesenchyme-specific *Setdb1* knock-out resulted in an increase of articular chondrocytes terminal differentiation.[10] Furthermore, Setdb1 is crucial for early neurogenesis in mice by promoting proliferation and cell survival.[11] In contrast, Setdb1 is crucial for osteoblast differentiation during bone development[12] and is involved in the terminal differentiation of skeletal muscle adult stem cells[13] and growth plate chondrocytes.[14]

As a H3K9 KMT, Setdb1 shows unusual distinct subcellular and subnuclear distributions, including in ESCs,[8,13,15–17] but the meaning of the different Setdb1 subcellular localizations remains mostly unknown. Although the role of nuclear Setdb1 in transcription regulation, especially in mESCs, has been extensively studied, its cytoplasmic role remains elusive.

Since Setdb1 is essential for ESCs, we first asked whether cytoplasmic Setdb1 (cSetdb1) is required for the survival of ESCs. Our cellular studies showed that the loss of a normal cytoplasmic localization of Setdb1 in ESCs lowers the cell number in time and increases the number of apoptotic cells. Biochemical protein-protein interaction studies unraveled that cSetdb1 interacts with several regulators of mRNA processing and translation, among which is the ESC-specific RNA binding protein (RBP) Trim71/Lin41. Proteomic studies

[1]Université Paris Cité, CNRS, Epigenetics and Cell Fate, UMR7216, 75013 Paris, France

[2]These authors contributed equally

[3]Lead contact

*Correspondence:
bertrand.cosson@u-paris.fr (B.C.),
slimane.aitsiali@u-paris.fr (S.A.-S.-A.)

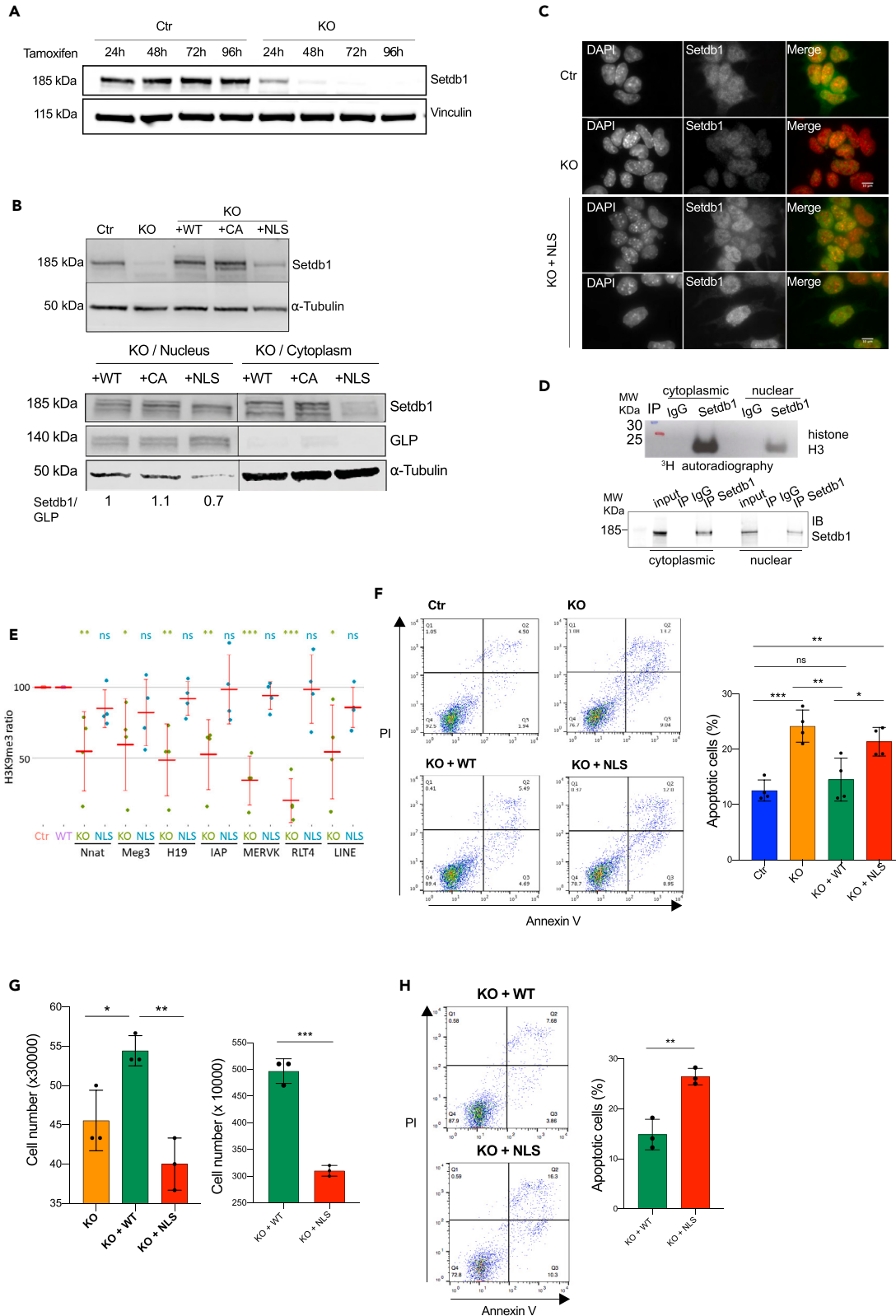https://doi.org/10.1016/j.isci.2023.107386

Figure 1. Cytoplasmic Setdb1 is essential for the survival of mESCs

(A) Setdb1 protein level in total protein extracts from ES cells (genetically modified TT2 cells, inducible for an acute *Setdb1* KO through Tamoxifen treatment). Setdb1 expression was analyzed in ES cells (Ctr) and *Setdb1* KO ES cells after 24 h, 48 h, 72 h, and 96 h of Tamoxifen treatment. Vinculin is used as loading control.

(B) *Upper panel*, Setdb1 expression was analyzed after 48-hour-Tamoxifen treatment in *Setdb1* KO ES cells. *Setdb1* inducible KO ES cells stably expressing wild-type Flag-Setdb1 (KO + WT), the enzymatically dead point mutant (KO + CA), or the nuclear-specific form of Flag-Setdb1 (KO + NLS), and in non-treated ES cells (Ctr). Vinculin or Tubulin is used as Western blot loading control. *Lower panel*, Setdb1 protein level obtained from nuclear/cytoplasmic fractionation. GLP is used as a nuclear extraction control; tubulin detection is used as a cytoplasmic extraction control. Setdb1 expression was analyzed in Ctr, KO, KO + WT, KO + CA, KO + NLS.

(C) Immunofluorescence using anti-Setdb1 antibody, performed in Ctr, KO and KO + NLS ES cells. Green: Setdb1; red: DAPI.

(D) *In vitro* radioactive methylation test using histone H3 within purified nucleosomes as substrate, radioactive S-Adenosyl Methionine (SAM) as methyl donor and immunoprecipitated Setdb1 from the cytoplasmic or nuclear fractions of mESCs. *Upper panel*, autoradiography; *lower panel*, Western blot.

(E) H3K9me3 level was analyzed for Setdb1 gene targets by ChIP-qPCR in Ctr, KO, KO + WT and KO + NLS cells. For each gene, the methylation level was expressed as a percentage of the level in Ctr cells for KO cells, and to KO + WT cells for KO + NLS cells and therefore was set to 100% for Ctr and KO + WT cells. The values represent the mean ± SD of four independent experiments. Statistic test: unpaired t-test *p value <0.1; **p value <0.05; ***p value <0.01; ns = not significant.

(F) Annexin V FITC Assay to detect apoptotic cells (Annexin V+/PI- and Annexin V+/PI + cells) in Ctr, KO, KO + WT, KO + NLS ES cells (*Setdb1* KO was obtained after 96 h of Tamoxifen treatment). FACS data: the quadrant on the lower left includes analyzed living cells (Annexin V-/PI-), the quadrant on the lower right includes cells in the early stage of apoptosis (Annexin V+/PI-), the quadrant on the upper right includes cells in the late stage of apoptosis (Annexin V+/PI+) and the quadrant on the upper left includes the cells in necrosis (Annexin V-/PI+). FACS data were quantified and represented as scatterplot with bars. N = 4. Statistic test: unpaired t-test *p value <0.05; **p value <0.01; ***p value <0.001; ns = not significant.

(G) Live cell number was determined in KO, KO + WT, KO + NLS (*Setdb1* KO was obtained with Tamoxifen treatment for 96h (left panel) or 120h (right panel)), using Trypan Blue staining assay. N = 3. Statistic test: t-test *p value <0.05; **p value <0.01.

(H) Left: Annexin V FITC Assay to detect apoptotic cells (Annexin V+/PI- and Annexin V+/PI + cells) in KO + WT, KO + NLS, after 5 days of Tamoxifen treatment. FACS data were quantified and represented as scatterplot with bars. N = 3. Statistic test: t-test **p value <0.01.

further demonstrated that cSetdb1 is required for the integrity of Trim71 protein complexes. In agreement with these results, the loss of cSetdb1 affects specific mRNA abundance and the overall rate of newly synthesized proteins. Taken together, our results unraveled an unknown fundamental role of cSetdb1 in mESCs, which influences gene expression regulation at the post-transcriptional level and provide new insights into the cytoplasmic regulation of gene expression mediated by a key epigenetic regulator.

RESULTS

Cytoplasmic Setdb1 is an active lysine methyltransferase required for the survival of embryonic stem cells

Setdb1 is essential for mouse embryonic stem cells survival (mESCs, see introduction). While Setdb1 function, extensively studied in mESCs, has been always associated with its nuclear role, it has been shown that Setdb1 also localizes in the cytoplasm. However, the importance and the function of cytoplasmic Setdb1 (cSetdb1) in mESCs has never been investigated.

To investigate the role of cytoplasmic Setdb1 in mESCs we sought to deplete the cSetdb1 while keeping normal nuclear Setdb1. To this end, we have first attempted to inactivate the two putative nuclear export signals (NES)[18] in the N-terminal part of Setdb1 by point mutations or deletion. However, Setdb1 NES mutation did not show any effect on Setdb1 subcellular localization (Figure S1), precluding the possibility of using this approach. Therefore, we used the TT2 mESCs which have been genetically modified to induce acute *Setdb1* knockout (KO) through tamoxifen treatment (TA),[19] in which an acute Setdb1 protein depletion was obtained from 48h post-TA treatment (Figure 1A). We used versions of these inducible TT2 *Setdb1* KO cells in which exogenous wild-type Setdb1 (KO + WT) or enzymatically dead point Setdb1 mutant (KO + CA) were stably expressed (Figure 1B), in the nucleus and in the cytoplasm. We next generated inducible *Setdb1* KO cells where WT Setdb1 expression is stably rescued only in the nucleus (KO + NLS) by adding to Setdb1 N-terminal part dual strong nuclear localization signal (NLS, detailed in the STAR Methods section) (Figures 1B and 1C).

Using these cell systems, we first investigated whether cSetdb1 is enzymatically active. To this end, we performed an immunoprecipitation (IP) of Setdb1 from the nuclear or cytoplasmic fractions of mESCs (Figure 1D), or from cytoplasmic fractions of Ctr, KO, KO + WT or KO + CA mESC lines (Figure S2A), using anti-Setdb1 antibody. We used the IP products in an *in vitro* radioactive methylation assay using core histones as a substrate and radioactive S-adenosyl methionine (SAM) as methyl donor. We observed an enzymatic activity toward H3 in nuclear but also cytoplasmic IPs (Figure 1D), and in the control cells

Ctr and KO + WT conditions, but not in KO and KO + CA (Figure S2A), as expected. Since the immunoprecipitates from KO and KO + CA cells do not show any detectable methyltransferase activity (Figure S2A), we deduced that previous detected signals were specific for Setdb1. Thus, we concluded that mESCs cSetdb1 is enzymatically active.

Next, we have checked that the NLS-Setdb1 form is also enzymatically active using the same experimental set up. Indeed, we have performed a radioactive methylation assay using different versions of Setdb1: WT, CA (i.e., catalytically inactive version) and NLS, immunoprecipitated from mESCs, as described in Figure 1D. These Setdb1 versions were purified from the nuclear fractions. Setdb1-NLS shows a significant and comparable enzymatic activity with WT Setdb1, in contrast to the enzymatically dead point CA mutant that displayed a barely detectable activity (Figure S2B). Note that the Sedtb1 classical WB doublets are not observed for NLS-Setdb1, suggesting an absence of the cytoplasmic localization of the Setdb1-NLS form (Figure 1B higher panel; Figure S2B and data not shown).

We then analyzed the H3K9 methylation status at classically described Setdb1-target regions (Figure 1E). As expected, in KO cells gene targets displayed reduced H3K9 trimethylation. No significant difference was observed between KO + WT and KO + NLS conditions, indicating that the NLS-Setdb1 version behave a similar activity compared with the WT version to mediate trimethylation of H3K9 in Setdb1-target regions. Consistently we did not observe significant differences between KO + WT and KO + NLS measuring the global level of H3K9me3 by Western blot (Figure S2C).

Moreover, transcriptomic data further confirmed that the NLS-Setdb1 fulfills the nuclear functions of Setdb1 (see below and Figure 4). Hence, we used this approach to deplete Setdb1 in the cytoplasm and study the biological consequences on mESCs. Thus, through these experiments, we validated a method to deplete Setdb1 specifically from the cytoplasm and we used this approach to study the biological consequences of cSetdb1 depletion in mESCs.

Setdb1 depletion is known to cause growth defects in ESCs,[20] but the importance of Setdb1 cytoplasmic function has never been specifically examined. To this end, we first performed an apoptosis test using Annexin V-FITC/IP staining in KO and KO+NLS-Setdb1 cells, compared to Ctr and KO + WT cells, after a long-term acute Setdb1 KO (96h of TA treatment, Figure 1F). As expected, we found almost twice more apoptotic cells in early stage (Annexin V+) and late stage (Annexin V+/Propidium Iodide-PI+) of apoptosis upon acute Setdb1 depletion (KO) compared to control (Ctr). Rescue of WT Setdb1 (KO + WT) restored the normal apoptotic index, while the expression of nuclear-only Setdb1 (KO + NLS), did not, showing an increase in the number of apoptotic cells. To go further, we quantified the number of attached cells, which are living (trypan blue-positive). In accordance with the previous result, we observed a significant decrease in the number of KO and KO + NLS attached cells, compared to control KO + WT cells (Figure 1G, left panel). To further check if cSetdb1 is essential in ESCs, we looked after 5-day of TA treatment. Our data showed that the increase in the number of apoptotic cells was even exacerbated when we express the nuclear-only Setdb1 (KO + NLS cells) obtained after 5 days of Tamoxifen treatment and the number of attached cells decreased (KO + NLS, Figure 1H, right panel). Moreover, an increase in cleaved caspase-3 was detected in KO cells (Figure S2D).

Together, these data highlighted the importance of cytoplasmic Setdb1 for ESCs survival.

Cytoplasmic Setdb1 interacts with Trim71, a mESC-specific regulator of gene expression

We next sought to identify the protein partners of cSetdb1 to get clues on its possible roles in the cytoplasm. To this end, we conducted a yeast two-hybrid assay (Y2H, performed by Hybrigenics Services, France) to identify potential cSetdb1 protein partners. In the Y2H assay we used as a bait the full-length WT mouse Setdb1 cDNA, screened against a mESC cDNA library. The Y2H showed an interaction between Setdb1 and its known co-factor ATF7IP (also called MCAF or mAM,[21]) with "very high confidence in the interaction" score, validating the approach. To further validate our results, we have confirmed by Y2H 1-to-1 experiment the interaction of Setdb1 with Mtr4/Skiv2l2, Pdcd10 and CDC23 (Figure S3), Trim71 (see below Figure 2A), and eIF3C (Figure S4A).

Interestingly, among the "very high or high confidence in the interaction" scores, the Y2H data showed that Setdb1 interacts with several regulators of mRNA stability and translation, including the Mtr4 RNA helicase
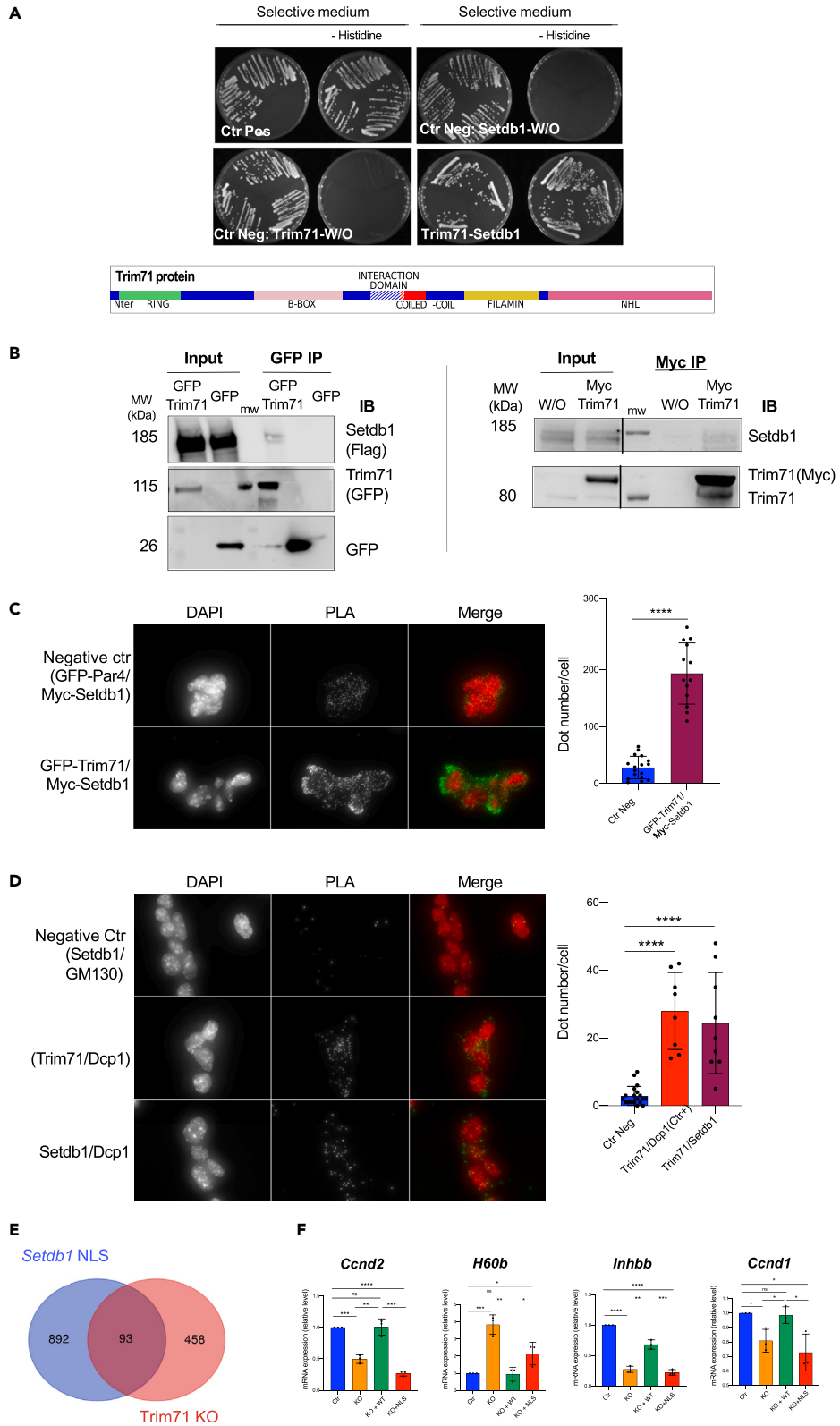
A

B

C

D

E

F

Figure 2. Cytoplasmic Setdb1 interacts with Trim71, a mESC-specific regulator of gene expression

(A) Top panel: Directed Yeast-two-hybrid test showing the interaction between Setdb1 and Trim71. Bottom panel: representation of the Trim71 major domains and the domain which mediates the interaction between Trim71 and Setdb1 (hatched white, aa 358–397).

(B) Co-Immunoprecipitation assay performed from the cytoplasmic fraction of ES cells stably expressing flagged WT-Setdb1 and transiently expressing GFP-Trim71 (on the left) or Myc-Trim71 (on the right). Trim71 was detected with anti-GFP (on the left) or anti-Myc or anti-Trim71 (on the right) antibodies and the co-immunoprecipitated Setdb1 was detected with anti-Flag (on the left) or anti-Setdb1 (on the right) antibodies. The plasmid expressing GFP (on the left) or the empty plasmid (on the right, W/O) were used as negative controls. MW: molecular weight marker.

(C) *In situ* proximity ligation assay using anti-Myc and anti-GFP antibodies, performed in ES cells transiently expressing Myc-Setdb1 and GFP-Trim71. ES cells transiently expressing Myc-Setdb1 and GFP-Par4 were used as negative control. Green: PLA signal. Red: DAPI. PLA signals were quantified (number of spots) and represented as scatterplot with bars. ****p value <0.0001.

(D) *In situ* proximity ligation assay using anti-Setdb1 and anti-Dcp1a performed in ES cells. Anti-GM130 was used as negative control Green: PLA signal. Red: DAPI. PLA signals were quantified (number of spots) and represented as scatterplot with bars. ****p value <0.0001.

(E) Venn diagram showing the numbers and the significant overlap (p value < 0.0001) of RNAs that are differentially abundant between KO + WT and KO + NLS (differentially expressed genes (DEGs) were selected for a logFC ≥ 1 and p value< 0.01) and differentially regulated genes after *Trim71*-KO.[27]

(F) RT-qPCR for endogenous *Ccnd2*, *H60b*, *Inhbb*, *Ccnd1* mRNAs performed in Ctr, KO, KO + WT, KO + NLS to validate RNAseq results. N = 3. Statistic test: t-test *p value <0.05; **p value <0.01; ***p value <0.001; ****p value <0.0001; ns = not significant.

(annotated as Skiv2l2 in Table S1), the RNA binding protein (RBP) Luc7l and the eukaryotic translation initiation factor eIF3C (annotated as 3230401O13Rik on Table S1).

Our Y2H data assigned a "very high confidence in the interaction" score to the interaction between Setdb1 and the major cytoplasmic RBP and mRNA silencer Trim71 (also called Lin41), specifically expressed in ESCs, which we confirmed in 1-by-1 Y2H assay (Figure 2A). We have confirmed the interaction between Setdb1 and eIF3C by Y2H 1-to-1 experiment (Figure S4A), a co-immunoprecipitation experiment from ESCs cytoplasmic extracts (Figure S4B), and PLA (Figure S4C). Interestingly, co-IP (Figure S4D) and PLA (Figure S4E) assays indicated proximity between eIF3C and Trim71 (Figure S4D). All in all, 6 interactors out of 14 that we found in our Y2H assay with high A-to-C scores have been also identified as Setdb1 partners by other methods, either in our present study (Trim71, eIF3C) or in previous ones (see Table S2). This includes Arl14ep, Atf7ip, Faf2 and Luc7l.

We next focused on the functional link between Setdb1 and Trim71. As Trim71 is a mESC-specific RBP localized the cytoplasm,[22] we assumed that the Setdb1/Trim71 functional interaction could take place in the cytoplasm. Trim71 has a double function: it is a E3 ubiquitin ligase and it regulates gene expression post-transcriptionally.[22–24] Notably, Trim71 localizes to Processing bodies (P-bodies), where mRNA repression occurs, and it is involved in the regulation of mRNA stability and translation.[22–24] The Y2H assay showed that the Setdb1/Trim71 interaction involves the coiled-coil domain of Trim71 (Figure 2A; Table S1), which is required for Trim71 to repress mRNA functions.[23] The interaction between Setdb1 and Trim71 was confirmed by co-immunoprecipitation of ectopically expressed proteins in mESCs (Figure 2B, left), and of exogenous Trim71 and endogenous Setdb1 (Figure 2B, right). Moreover, *in situ* interaction assay (Proximity Ligation Assay or PLA) confirmed that cSetdb1 interacts with Trim71 *in situ* in mESCs, strengthening our findings (Figure 2C, Video S1).

All together, these data showed an unprecedented interaction between a major epigenetic regulator Setdb1 and the key cytoplasmic RNA regulator Trim71.

Integrity of Trim71 complex(es), involved in mRNA stability and translation, is affected in the absence of Setdb1

Since Trim71 and Setdb1 are both enzymes (E3 ubiquitin ligase and lysine methyltransferase, respectively), we wondered whether their interaction may affect their reciprocal stability. Our data showed that acute *Setdb1* depletion (KO) did not affect Trim71 protein level, neither that of its known partner Ago2 (Figure S5A). Reciprocally, depletion of endogenous Trim71 (Trim71 knockdown or KD) did not affect Setdb1 protein level neither (Figure S5B).
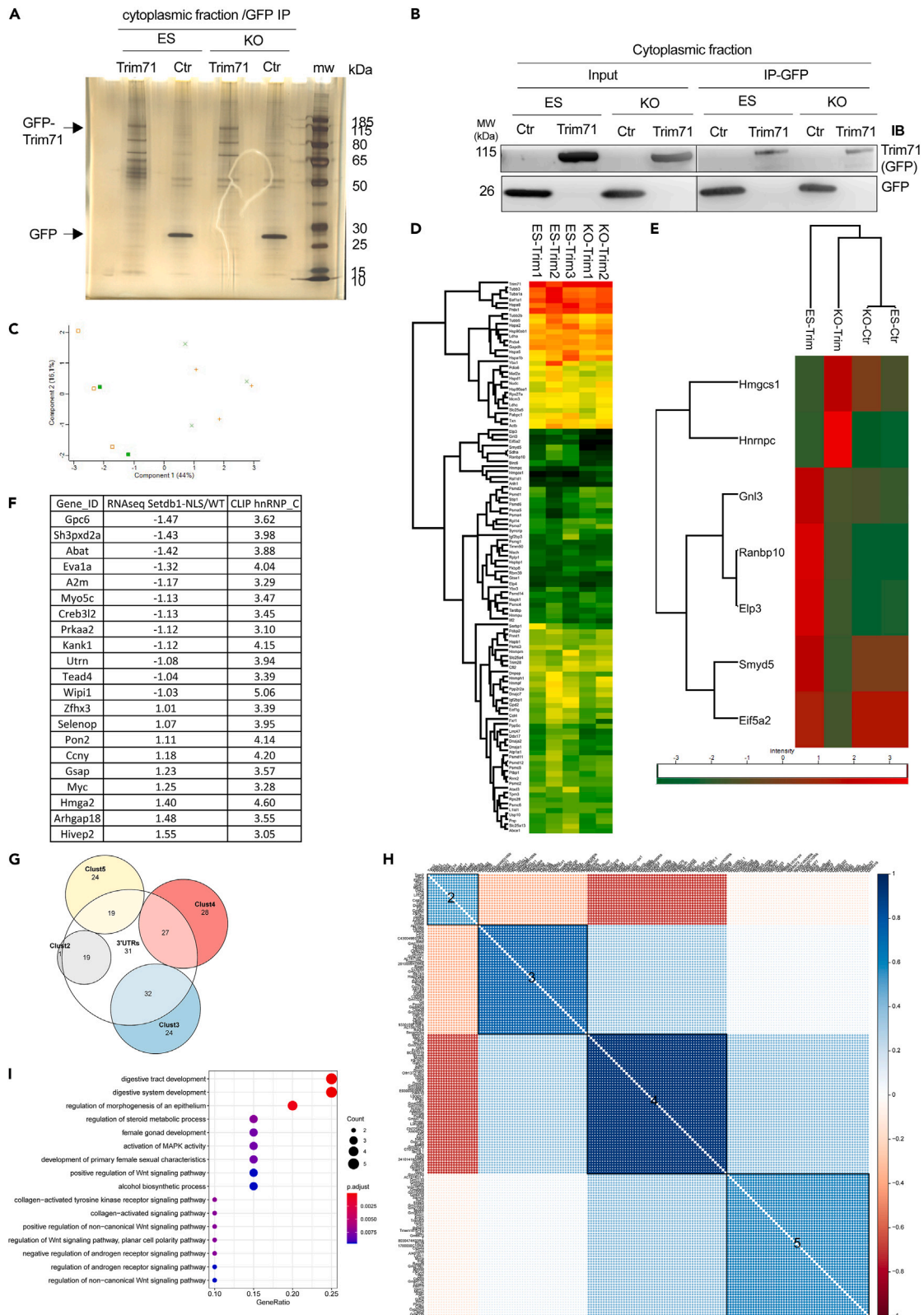
CellPress
OPEN ACCESS

A

cytoplasmic fraction /GFP IP

ES		KO		
Trim71	Ctr	Trim71	Ctr	mw	kDa

GFP-Trim71 →

185
115
80
65
50

GFP →

30
25

15
10

B

Cytoplasmic fraction

	Input				IP-GFP				IB
	ES		KO		ES		KO		
MW (kDa)	Ctr	Trim71	Ctr	Trim71	Ctr	Trim71	Ctr	Trim71	
115									Trim71 (GFP)
26									GFP

C

Component 2 (16.1%) / Component 1 (44%)

D

ES-Trim1, ES-Trim2, ES-Trim3, KO-Trim1, KO-Trim2

E

ES-Trim, KO-Trim, KO-Ctr, ES-Ctr

Hmgcs1
Hnrnpc
Gnl3
Ranbp10
Elp3
Smyd5
Eif5a2

intensity

F

Gene_ID	RNAseq Setdb1-NLS/WT	CLIP hnRNP_C
Gpc6	-1.47	3.62
Sh3pxd2a	-1.43	3.98
Abat	-1.42	3.88
Eva1a	-1.32	4.04
A2m	-1.17	3.29
Myo5c	-1.13	3.47
Creb3l2	-1.13	3.45
Prkaa2	-1.12	3.10
Kank1	-1.12	4.15
Utrn	-1.08	3.94
Tead4	-1.04	3.39
Wipi1	-1.03	5.06
Zfhx3	1.01	3.39
Selenop	1.07	3.95
Pon2	1.11	4.14
Ccny	1.18	4.20
Gsap	1.23	3.57
Myc	1.25	3.28
Hmga2	1.40	4.60
Arhgap18	1.48	3.55
Hivep2	1.55	3.05

G

Clust5 24
Clust4 28
Clust2 19
3'UTRs 31
19
27
Clust3 24
32

H

I

digestive tract development
digestive system development
regulation of morphogenesis of an epithelium
regulation of steroid metabolic process
female gonad development
activation of MAPK activity
development of primary female sexual characteristics
positive regulation of Wnt signaling pathway
alcohol biosynthetic process
collagen−activated tyrosine kinase receptor signaling pathway
collagen−activated signaling pathway
positive regulation of non−canonical Wnt signaling pathway
regulation of Wnt signaling pathway, planar cell polarity pathway
negative regulation of androgen receptor signaling pathway
regulation of androgen receptor signaling pathway
regulation of non−canonical Wnt signaling pathway

Count
2, 3, 4, 5

p.adjust
0.0025, 0.0050, 0.0075

GeneRatio

Figure 3. Integrity of Trim71 complex(es), involved in mRNA stability and translation, is affected in the absence of Setdb1

(A and B) GFP-Trim71 (Trim71) was immunoprecipitated from the cytoplasmic fractions of control or *Setdb1* KO ES cells. GFP (Ctr) was used as a control of the immunoprecipitation. (A) Silver staining to detect proteins of immunoprecipitated proteins. (B) The amount of immunoprecipitated proteins Trim71 and GFP in ES or KO cells was checked by western blot.

(C) PCA analysis. ES-Ctr (orange cross), KO-Ctr (green diagonal cross), ES-Trim71 (orange square), KO-Trim71 (green filled square).

(D) Differential analysis (multiple sample test ANOVA) after quantification of almost 800 proteins of which 108 are differentially enriched at FDR <0.1 level. Heatmap after clustering of these significant proteins with the sum of their intensities.

(E) Heatmap after clustering of the significant proteins with the score obtained by the Tukey's honestly significant difference with an FDR <0.05 (THSD, B).

(F) List of gene names of the mRNAs that are differentially expressed in KO + WT and found associated to hnRNP-c by eCLIP, see text for details. Number refers to LogFC.

(G) Clustered correlation plot of the 291 differentially abundant mRNAs reveals 4 distinct co-expressed modules. Soft-thresholded correlation matrix of the 291 DEG TPMs clustered by hierarchical clustering and the Ward D2 linkage identifies the structure of 5 modules (the 5th module containing the rest 117 DEGs with relatively low correlation, was excluded from the figure). Each module represents a set of co-expressed genes which might also be co-regulated.

(H) Venn diagram showing the clusters of the 157 mRNAs differentially abundant in absence of cSetdb1 function and the mRNAs whose 3′UTR are potential binding site of hnRNP-C (white circle).

(I) GO enrichment DotPlot of the second co-expressed module (Cluster 2) of the correlation plot of panel H. Enrichment identifies GO categories related to MAPK activation and WNT signaling. Again (like in Figure 4) categories are sorted according to GeneRatios and color and size correspond to the corrected p value and the gene count for each category.

Thus, to better understand the functional relation between Setdb1 and Trim71, we wondered whether Setdb1 is essential for the integrity of Trim71 complex and Trim71 capacity to interact with its partners, therefore for its functions. To address this, we performed a proteomic analysis on Trim71 complex(es) in absence of Setdb1. We immunoprecipitated (IP) the cytoplasmic GFP-tagged Trim71 (Trim71) and its specific partners in control ESCs (ES) or in ESCs where we acutely depleted *Setdb1* after 48h of tamoxifen treatment (KO), a timepoint which does not alter the viability, neither proliferation, size and granularity of the cells, rRNAs level or RNA synthesis (shown in Figures S6A–S6E). We compared the 2 GFP-Trim71 IPs performed in Ctr and KO ES cells (Figures 3A and 3B). Of note, Setdb1 and Trim71 protein levels are not interdependent (Figures S5A and S5B). The purified Trim71 complexes were analyzed by mass spectrometry. After discarding the sample with low sum of intensity (Figure S7A), we filtered for proteins that were well represented in the immunoprecipitates; we then applied a scale to interval normalization to better compare the samples (see STAR Methods). As expected, the PCA analysis (Figure 3C) separates well all Trim71 samples (GFP-Trim) from all control (Ctr) samples (GFP). We then performed an ANOVA multi-sample test, which ended to the selection of 108 proteins that were found differentially present in at least 2 of the 4 conditions (Figure 3D).

In order to select the protein partners of Trim71 that could differentially bind to Trim71 after an acute *Setdb1* knockout (KO-Trim71 against ES-Trim71), we performed a Post-Hoc Tukey's HSD test. We found, as displayed on the heatmap (Figure 3E), that some Trim71 partners are more or less associated with Trim71 in absence of Setdb1 (KO-Trim71) compared to control cells (ES-Trim71). Notably, the RNA-binding protein hnRNP-C and Hmgcs1 are more enriched in KO-Trim71 compared to ES-Trim71. Conversely, Eif5a2, Elp3, Gnl3, Ranbp10 and Smyd5 are less enriched in KO-Trim71 compared to ES-Trim71. Very interestingly, these proteins are mainly involved, and associated with, mRNA stability, ribosome biogenesis and translation regulation. Furthermore, we have crossed the list of these Trim71-interacting proteins (Figure 3E) and did not find any of them in the differentially expressed genes identified by RNAseq between WT and Setdb1 KO cells (even with a log2FC threshold of 1, p < 0.01, cf. Table S3). Thus, these data illustrated that the profile of Trim71 partners, whereby Trim71 executes its cellular functions, is at least partly dependent on Setdb1 and provided important mechanistic hypothesis of a possible role of cSetdb1 in post-transcriptional regulation.

Altogether, these observations shed new light on Trim71 complex function in mRNA stability and translation and reveals the importance of Setdb1 in Trim71 complex architecture, confirming the intimate relation between Setdb1 and Trim71.

Cytoplasmic Setdb1 is required for normal mRNA abundance

Our data showed that Setdb1 is a cytoplasmic partner of the ESC-specific RBP and mRNA silencer Trim71/Lin41. The Setdb1/Trim71 interaction involves the coiled-coil domain of Trim71 (Figure 2A; Table S1), which also directs Trim71 to P-bodies, where mRNA repression occurs.[24] Furthermore, using PLA, we have also observed a spatial proximity between Trim71 and DCP1a (Figure 2D), a mRNA decapping enzyme involved in mRNA stability known to co-localize with Trim71. Altogether, the PLA results indicate a direct interaction
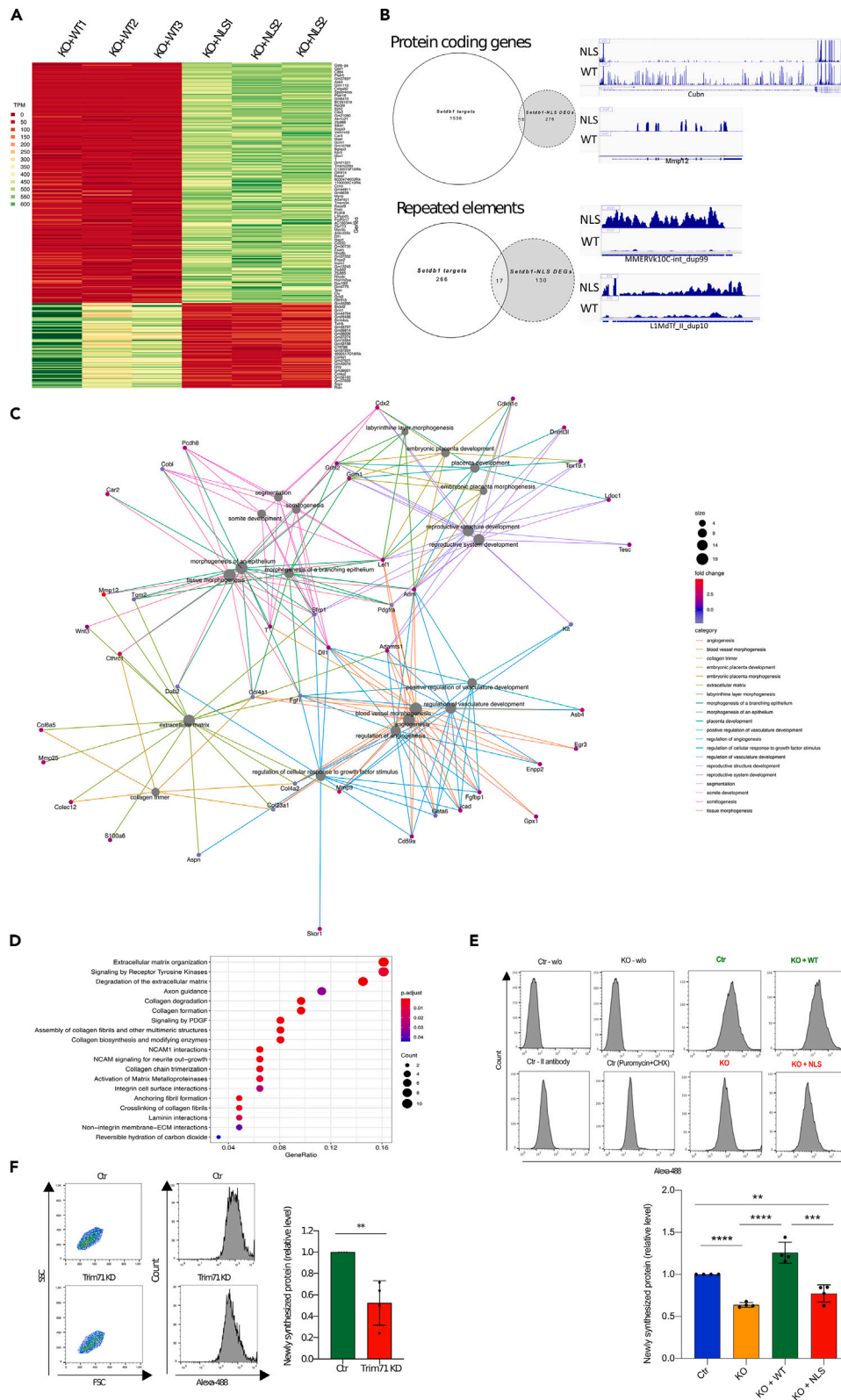
A

KO+WT1 KO+WT2 KO+WT3 KO+NLS1 KO+NLS2 KO+NLS2

TPM
0
50
100
150
200
250
300
350
400
450
500
550
600

B

Protein coding genes

Setdb1 targets 1538 — Setdb1-NLS DEGs 279

Repeated elements

Setdb1 targets 266 — 17 — Setdb1-NLS DEGs 130

NLS / WT — Cubn

NLS / WT — Mmp12

NLS / WT — MMERVk10C-int_dup99

NLS / WT — L1MdTf_II_dup10

C

size
4
9
14
19

fold change
2.5
0.0

category
angiogenesis
blood vessel morphogenesis
collagen trimer
embryonic placenta development
embryonic placenta morphogenesis
extracellular matrix
labyrinthine layer morphogenesis
morphogenesis of a branching epithelium
morphogenesis of an epithelium
placenta development
positive regulation of vasculature development
regulation of angiogenesis
regulation of cellular response to growth factor stimulus
regulation of vasculature development
reproductive structure development
reproductive system development
segmentation
somite development
somitogenesis
tissue morphogenesis

D

Extracellular matrix organization
Signaling by Receptor Tyrosine Kinases
Degradation of the extracellular matrix
Axon guidance
Collagen degradation
Collagen formation
Signaling by PDGF
Assembly of collagen fibrils and other multimeric structures
Collagen biosynthesis and modifying enzymes
NCAM1 interactions
NCAM signaling for neurite out-growth
Collagen chain trimerization
Activation of Matrix Metalloproteinases
Integrin cell surface interactions
Anchoring fibril formation
Crosslinking of collagen fibrils
Laminin interactions
Non–integrin membrane–ECM interactions
Reversible hydration of carbon dioxide

GeneRatio

p.adjust
0.01
0.02
0.03
0.04

Count
2
4
6
8
10

E

Ctr - w/o | KO - w/o | Ctr | KO + WT
Ctr - II antibody | Ctr (Puromycin+CHX) | KO | KO + NLS

Count — Alexa-488

Newly synthesized protein (relative level)
Ctr | KO | KO + WT | KO + NLS

F

Ctr | Ctr
SSC / FSC | Count / Alexa-488
Trim71 KD | Trim71 KD

Newly synthesized protein (relative level)
Ctr | Trim71 KD

Figure 4. Cytoplasmic Setdb1 regulates the abundance of mRNAs and newly synthesized proteins

(A) K-means clustering (k = 2) of the normalized transcripts per million (TPM) of all the 291 differentially expressed genes (DEGs). DEGs were selected for a logFC ≥ 1.5 and p value < 0.01. On the plot their expression levels in the three KO + WT and the three KO + NLS samples are highlighted, with red highlighting low and green highlighting high expression level. The two groups of DEGs are clearly separated and these two are the only two robust clusters obtained by k-means clustering.

(B) The differentially regulated genes in Setdb1-NLS do not overlap with the Setdb1-bound genes in the mESCs. Setdb1 direct target genes from the ChIP-Seq data (purple circle) of a landmark publication ([6]; Table S4) were intersected with the 291 DEGs from coding genes we found from our Setdb1-NLS RNA-Seq data (green circle). The same was done for transcripts from repeated elements (blue and red circles). The overlap of these two sets was not significant (only 15 and 17 genes respectively for coding genes and repetitive elements, expected number >20, p value >0.1). Right panels: genome browser (IGV) screenshots of some differentially regulated RNAs, either from coding genes (upper part) or repeated elements (lower part).

(C) Category Network plot (cnetplot) of the top 20 enriched terms from the gene ontology biological processes. Cnetplots represent relationships between biological concepts (here GO Biological Processes) and the genes contained in them. Each different concept link is highlighted with different colors. The size of circles corresponds to the concept enrichment and the green-red gradient for each gene represents its log fold change.

(D) DEGs pathway enrichment. DotPlot diagram for pathway enrichment of differentially expressed genes in KO + NLS compared to KO + WT (Fold change >1.5, p value <0.01). Pathways are sorted according to the ratio of the number of DGEs found in each pathway over the number of genes in such pathway (GeneRatio horizontal axis). The color of each circle corresponds to the -corrected for multiple testing-p value of the enrichment test and the size of each circle is equivalent to the number of DEGs found in each pathway.

(E) SUnSET experiment performed in Ctr, KO, KO + WT and KO + NLS. Setdb1 KO condition correspond to 48 h of Tamoxifen treatment. Cells were treated with 1 μg/mL Puromycin for 20 min, then analyzed by FACS after the addition of anti-puromycin antibody and a fluorescent secondary antibody. Several experimental controls were used: cells without any treatment and any antibodies labeling (Ctr-w/o; KO-w/o), cells labeled only with the secondary antibody in order to detect the experiment background (Ctr - II antibody); cells treated with both Puromycin and Cycloheximide, a translation inhibitor (Ctr (Puromycin + CHX)) as negative control. FACS data were quantified (using the median values) and represented as scatterplot with bars. N = 4. Statistic test: t-test *p value <0.05; **p value <0.01; ***p value <0.001; ns: not significant.

(F) SUnSET experiment performed as in E in Ctr and Trim71 KD cells. Trim71 KD was obtained after 72 h of siRNA treatment. N = 4. Statistic test: t-test **p value <0.01.

through physical contact or close functional coupling between Setdb1, Trim71 and DCP1a (Figures 2D and S5C, Video S2). These results suggested a potential functional link between Setdb1, Trim71 and DCP1a to regulate mRNA behavior in ESCs.

Therefore, we wondered whether cSetdb1 could influence gene expression at post-transcriptional level considering the importance of such regulation for the protein abundance and ESC identity.[1,25] First, we checked the amount of single mRNAs in KO + NLS compared to KO + WT mESCs cells by RNAseq, after ribodepletion. First, the PCA analysis showed that the KO + NLS triplicates were well defined and appear to form a distinct group from the KO + WT triplicates (Figure S6F). 291 mRNAs were found differentially abundant in KO + NLS compared to KO + WT cells (Figures 4A and 4B upper panels; Table S3); of those genes, 76 were less abundant and 215 more abundant. While the role of Setdb1 in regulating gene expression has been always associated with its nuclear roles, our RNA-seq data suggest that cytoplasmic Setdb1 is also involved in gene expression regulation, at the mRNA abundance level. We have also analyzed the abundance of transcripts from repetitive elements and found 147 differentially regulated repeats in KO + NLS compared to KO + WT cells (Table S4; Figure 4B lower panels).

We have crossed our differentially abundant RNAs in the KO + NLS versus KO + WT ESCs identified by RNA-seq with the Setdb1 direct target genes obtained by ChIP-seq in the same ESCs.[6] We did not find a significant overlap between the two lists according to a hypergeometric distribution test (Figure 4B, left panels), suggesting that cytoplasmic and nuclear functions of Setdb1 are separated since they regulate different sets of genes, both for coding genes and for transcripts from repetitive sequences.

Gene ontology (GO) analysis for biological processes showed that most of the differentially abundant mRNAs are enriched in gene categories related to Setdb1-dependent phenotypes in mice (summarized in: http://www.informatics.jax.org/marker/MGI:1934229). Notably, embryogenesis, including development (vascular, reproductive, placenta and somite development), tissue morphogenesis (including also branchial, epithelial and placenta morphogenesis), segmentation and regulation of cellular response to

growth factor stimuli (Figure 4C). In particular, we identified more abundant mRNAs related to reproductive and placenta development (such as *Gcm1* and *Tex19.1*) and to vascular, vessel development and angiogenesis (such as *Gpx1, Egr3, Adm* and *Enpp2*). Moreover, in line with the phenotype that we observed in absence of cSetdb1 (KO+NLS-Sedtb1 cells), we found less abundant mRNAs associated with cell proliferation and cell survival, including *Dab2, kit, Fgf1* and *Pdgfra* (Figure 4C). Furthermore, enrichment analysis for biological processes and pathways showed that the differentially abundant mRNAs are enriched in categories related to extracellular matrix (ECM), including ECM organization, collagen formation and multimerization, and cell adhesion (Figure 4D). In particular, we identified less abundant mRNAs related to ECM structure/organization (such as collagen genes *Col23a1, Col4a1,* and *Col4a2*) and more abundant mRNAs related to ECM degradation (such as the matrix metalloproteinases *Mmp12, Mmp9* and *Mmp25*) as already shown.[26] All these categories and pathways are notably involved in ESCs self-renewal, proliferation, and differentiation, thus associated with ESCs identity and integrity. Interestingly, in accordance with the enrichment analysis, KO+NLS-Setdb1 ESCs showed more spread distribution and less compact clones compared to KO + WT-Setdb1 control ESCs, a phenotype reminiscent of more committed cells (Figure S6G).

All these data show that in mESCs cytoplasmic Setdb1 affects the abundance of mRNAs mainly involved in development and cell adhesion and suggest a loss of the stemness traits and a potential acquisition of a differentiated phenotype upon depletion of Setdb1 cytoplasmic functions.

Cytoplasmic Setdb1 and Trim71 co-regulate the abundance of a subset of mRNAs

We next evaluated the functional significance of the cSetdb-Trim71 interaction by checking if Trim71-regulated mRNAs are also dependent on cSetdb1. Comparing our RNA-seq results (described in Figure 4A) with the transcripts differentially regulated after *Trim71* knock-out in mESCs,[27] we found 93 mRNAs commonly regulated by cSetdb1 (Setdb1 NLS) and Trim71 (*Trim71* KO) (Figure 2E), 18 of them linked to multicellular organismal reproductive process (top biological process category from our ontology analysis (in bold in: Table S3, right sheet - log2FC threshold of 1). Thus, we wondered whether cSetdb1 could influence the abundance of selected Trim71 mRNA targets, mainly involved in cell proliferation and embryogenesis, including *Inhbb* and *Ccnd2* and potential Trim71 targets, including *H60b* and *Ccnd1*. Both by RNA-seq and RT-qPCR we found all these 4 mRNAs dysregulated in absence of *Setdb1* (KO) or upon the expression of the nuclear-specific Setdb1 (KO + NLS), compared to the controls (Ctr and KO + WT) (Table S3; Figure 2F). Our data show that cSetdb1 and Trim71 co-regulate the abundance of common mRNAs.

Our proteomic data showed here for the first time that the RBP hnRNP-C, known to be involved in mRNA turnover and translation, is in complex with Trim71 (Figure 3D). Furthermore, we found that hnRNP-C associates more with Trim71 in absence of cSetdb1 (Figure 3E), highlighting a Setdb1-dependent interaction between hnRNP-C and Trim71. Therefore, we wondered whether there is a functional correlation between cSetdb1 and hnRNP-C; we checked if some of the cSetdb1-dependent mRNAs are targets of hnRNP-C. We found 21 of the mRNAs found associated to hnRNP-C by eCLIP assay[28] are among the mRNAs differentially abundant in absence of cSetdb1 (Figure 3F). Interestingly, 6 of them are implicated in the Wnt signaling pathway, notably *GPC6, KANK1, CCNY, PRKAA2, HMGA2,* and *Myc*. The last three are also implicated in cell-cycle arrest. C-Myc is a known transcription factor, required for ESC self-renewal, maintenance of mESC identity and iPSC reprogramming.

In addition to eCLIP assay, the scanning of all mice 5′ and 3′UTRs for hnRNP-C hits, through an established online prediction tool RBPmap, has identified that both the mouse and the human Myc as a hnRNP-C target through its 5′UTRs (Figure S7B). It has been shown that hnRNP-C binds human c-Myc mRNA on 5′UTR, regulating *c-Myc* mRNA translation level.[29] We hypothesize that cSetdb1 would influence the c-Myc levels through hnRNP-C. In conclusion, we found interesting mRNAs regulated by cSetdb1 that are also hnRNP-C targets, strengthening our hypothesis concerning the functional correlation between hnRNP-C, Trim71 and cSetdb1 in post-transcriptional regulation.

Finally, we performed a predictive analysis to check for the binding profile of hnRNP-C on the mRNAs regulated by cSetdb1 (mRNAs described in Figure 4A; Table S3). Indeed, having a well characterized hnRNP-C RNA binding motif, we performed a stringent computational prediction using RBPmap (see STAR Methods), to scan the 5′ and 3′UTRs of the 291 differentially abundant mRNAs found in absence of

cytoplasmic Setdb1 for hnRNP-C binding target motifs. Out of the 157 3'UTRs that we managed to retrieve from ENSEMBL (STAR Methods), most of them (128) were identified as potential targets of hnRNP-C (Table S5).

Moreover, we clustered the gene expression correlations of all the 291 differentially abundant mRNAs that we found in our RNAseq in absence of cytoplasmic Setdb1. Clustering of the correlation coefficients of gene expression profiles of all 291 DEGs identified 5 distinct clusters with 4 of them demonstrating significant correlations and forming 4 distinct co-expressed modules (Figure 3G; Table S6). The diagram in Figure 3G indicates that the 20 differentially abundant mRNAs in cluster 2 (the first that appears on the Figure 3G diagram) are highly correlated between them and highly anti-correlated with the rest of the inferred clusters and therefore they bare the most informative signal, which might provide possible mechanistic links to the observed cellular phenotypes (Figures 1F–1H and S2D).

Remarkably, all mRNAs in cluster 2 (except one) were predicted as hnRNP-C targets (Figure 3H) and are less abundant in the absence of cSetdb1 function (Table S3). Furthermore, in line with the observed mESCs survival phenotype (Figure 1), downstream analysis of GO enrichment identified proliferation-related categories, notably Wnt signaling pathway and MAPK activity, including key genes (such as *Dab2* and *Dixdc1*) (Figure 3I). Interestingly, among the 20 transcripts of cluster 2, 5 (*Col4a2*, *Kit*, *Gata6*, *Zfp521*, *Ly75*) belong to the DEGs obtained after *Trim71* KO[30] (with FC +/−1.5 and hypergeometric 2.6×10^{-7}).

All these data analyses and predictions showed that hnRNP-C, one of the Trim71 partners that we found more associated with Trim71 in the absence of cSetdb1, targets almost half of the mRNAs that we found differentially abundant upon cSetdb1 depletion and provide a potential molecular mechanism through which cSetdb1 regulates gene expression post-transcriptionally. Overall, our proteomic results, the enrichments and the human/mouse UTR conservation, suggested that Setdb1 affects the integrity and the function of Trim71 complex, is responsible for the regulation of major pathways, and is involved in mESC survival and identity.

Altogether, these data confirm the previously demonstrated role of Trim71 in the regulation of mRNAs stability and translation, and highlights a functional role of cSetdb1, associated to Trim71, in post-transcriptional regulation of gene expression.

Cytoplasmic Setdb1 and Trim71 are both required for normal protein neo-synthesis

To deepen the study of cSetdb1 role in post-transcriptional gene expression control, we checked its potential participation in protein translation regulation. Although Setdb1 was shown to be associated with ribosomes,[31] Setdb1 possible role in translation regulation has not been investigated. Moreover, we found that cSetdb1 interacts with translation initiation factors (Table S1). To this end, we performed a SUnSET assay, which is a non-radioactive method to quantify the amount of newly synthesized proteins[32] that mirrors ongoing protein synthesis through puromycin incorporation. We acutely depleted *Setdb1* in ESCs after 48h of tamoxifen treatment, a timepoint which does not alter the viability (Figure S6A), neither proliferation (Figure S6B), size and granularity of the cells (Figure S6C), rRNAs level (Figure S6D) or RNA synthesis (Figure S6E). The SUnSET assay specifically showed that an early acute *Setdb1* depletion (KO) affects ongoing protein synthesis, revealing a statistically significant almost 40% decrease in the amount of newly synthesized proteins, compared to control cells (Ctr) (Figure 4E). This phenotype is rescued by WT Setdb1 in KO + WT ESCs. However, very interestingly, the expression of nuclear-only Setdb1 in KO + NLS ESCs did not rescue the protein synthesis defect, showing a statistically significant 42% decrease in the amount of newly synthesized proteins in KO + NLS compared to KO + WT ESCs (Figure 4E). Of note, the overall level of proteins does not significantly change in KO + NLS versus KO + WT ESCs when normalized to cell number, as the NLS/WT total protein amount ratio is 1.11 (n = 3, SD 0.02), from cytoplasmic, nuclear or total extraction normalized to cell number.

Since we found that cSetdb1 interacts with Trim71 and that Trim71 is associated with proteins involved in ribosome biogenesis and translation regulation, we wondered whether Trim71 could regulate the amount of newly synthesized proteins. Interestingly, the amount of newly synthesized proteins decreases in absence of Trim71 (Trim71 KD), compared to control (Ctr) (Figure 4F). Our results show the involvement of Trim71 in ongoing protein synthesis in mESCs as for cSetdb1.

Together, the SUnSET assay and the rescue experiments suggest that the loss of Setdb1 in the cytoplasm affects the amount of newly synthesized proteins, therefore that cSetdb1 is required for protein synthesis in mESCs.

Altogether, our RNA-seq data, enrichment analyses, and protein neo-synthesis showed that cytoplasmic Setdb1 plays key roles in post-transcriptional regulation of gene expression in ESCs, influencing mRNA abundance, and the synthesis of proteins.

DISCUSSION

The major H3K9 lysine methyltransferase Setdb1 (mouse Eset) is required for the maintenance and the normal growth of mESCs.[7,20] *Eset* KO embryos lack normal inner cell mass (ICM), do not form the epiblast, and the extra-embryonic trophectoderm is not affected.[5] Indeed, the inactivation of the mouse gene encoding Setdb1 (*Eset*) induces de-repression of differentiation genes caused by the loss of H3K9 methylation, in particular the trophectoderm genes, inducing the loss of ESC identity. These nuclear roles of Setdb1 in mESCs are thus well studied. However, Setdb1 is localized both in the nucleus and cytoplasm where we showed that it is enzymatically active. Our study addressed the potential cytoplasmic role of Setdb1 in mESCs. To this end, we have set a cellular system in which the cytoplasmic fraction of Setdb1 was depleted while the nuclear one was maintained. Overall, we found that the cytoplasmic function of Setdb1 is required for the survival and the normal growth of mESCs. This indicates that cytoplasmic Setdb1 (cSetdb1) regulates ESCs fate independently of its nuclear role.

Next, we asked whether cSetdb1 could regulate gene expression at the post-transcriptional level. Indeed, not only transcription regulation but also post-transcriptional regulations are both fundamental in ESCs fate and identity control.[1,25,33] Since Setdb1 has been shown to be associated with ribosomes,[31] we first checked whether cSetdb1 could influence protein synthesis. Our data showed that loss of cytoplasmic Setdb1 in mESCs results in a considerable decrease in global ongoing protein synthesis. This was further supported by our proteomic study showing a physical association of Setdb1 with several translational regulators in mESCs. Our data unravel an unsuspected role of Setdb1 in protein synthesis regulation in mESCs. Moreover, the considerable level of protein synthesis dysregulation, observed in early cSetdb1 loss-of-function (LOF) timepoint, may be the potential cause of cell death. Moreover, we asked whether cSetdb1 could regulate mRNA abundance. While the LOF of cSetdb1 function did not induce a significant change in the total mRNA levels, it induced changes in the abundance of specific mRNAs involved in embryogenesis, including development (vascular, reproductive, placenta, and somite development), tissue morphogenesis (including also branchial, epithelial, and placenta morphogenesis), segmentation and regulation of cellular response to growth factor stimuli. Thus, in addition to the well-described role of Setdb1 in regulating gene expression in the nucleus via H3K9 methylation, cSedtb1 seems to be crucial in mRNA abundance regulation in the cytoplasm independently of gene transcription.

As for RNA molecules recognition by cSetdb1, Setdb1 protein does not contain any RNA recognition motif (RRM). However, our proteomic data presented here showed a strong interaction between Setdb1 and many RBPs (Trim71, eIF3c, Mtr4/Skiv2l2). Thus, Setdb1 could indirectly interact with RNA through its RBP partners. In addition, an ongoing study in our lab (unpublished) to exhaustively characterize the Setdb1-dependent lysine methylome that unraveled many translation and RNA regulators to be differentially methylated in the absence of Setdb1, including eIF3c and Skiv2l2 that were also found in our Y2H screen (Table S1), and Chtop protein (chromatin target of PRMT1 protein) that belongs to the TREX complex (TRanscription-EXport), involved in RNA export to the cytoplasm. Chtop is known to interact with KMTs, such as SET1, in a methylation-dependent manner.[34] In addition, TREX action in mRNA nuclear export depends on m6A methylation (N^6-Methyladenosine),[35] and 5-methylcytidine is key in mRNA export since it is bound by the TREX subunit ALYREF.[36] Thus, we can propose a model in which SETDB1 could recognize methylated mRNA in the cytoplasm through its putative MBD (Methyl-CpG-binding domain) in order to methylate and regulate Chtop/TREX. Indeed, it has been shown that MDB-containing proteins, such as MDB2 and MeCP2, are able to bind RNA,[37] in addition to methylated DNA.

Our proteomic study showed that Setdb1 strongly interacts with the RNA-binding protein Trim71, a cytoplasmic key post-transcription regulator in ESCs. Trim71, which is both an E3 ubiquitin ligase and a mRNA silencer, co-localizes with DCP1a in P-bodies,[38,39] and is required for ESCs self-renewal.[22,40]

Interestingly, cSetdb1 and Trim71 regulate the abundance of common mRNAs and Trim71 LOF induces a similar effect on global protein synthesis as Setdb1 LOF does. These data illustrate the complementary roles and the functional relations that cSetdb1 and Trim71 have in mESCs.

Setdb1 LOF induced significant changes in Trim71 complex composition, including the presence of many proteins that are involved in mRNA stability and translation: hnRNP-C (RNA-binding protein involved in mRNA turnover and translation, among its different functions, Eif5a2 (translation elongation factor, involved also in mRNA turnover in addition to translation), Gnl3 (associated with proteins responsible of ribosome biogenesis), and Smyd5 (associated with the RNA helicase Mov10, a key protein involved in mRNA silencing together with the RISC complex[41]). These data illustrate that the profile of Trim71 partners, whereby Trim71 executes its cellular functions, is dependent on Setdb1 and provide important mechanistic hypothesis to explain the role of cSetdb1 in post-transcriptional regulation of gene expression, through Trim71.

The top Trim71 partner, whose interaction depends on cSetdb1, is the heterogeneous nuclear ribonucleoprotein hnRNP-C, which is also localized in the cytoplasm where it regulates the translation efficiency of specific mRNAs.[29,42] Interestingly, an interaction between Setdb1 and another member of the hnRNP family in the nucleus, hnRNP-K, has been already shown.[21] We observed that more hnRNP-C protein interacts with Trim71 in cSetdb1 LOF condition. Thus, cSetdb1 is essential for a balanced and harmonious interaction between hnRNP-C and Trim71. Moreover, cSetdb1 and hnRNP-C share common mRNA targets. Interestingly, previous studies showed that the human hnRNP-C binds *c-myc* mRNA[28,29] in particular on its 5'UTR,[28] enhancing c-Myc translation in a global context of partial translation inhibition.[29] The scanning of all mice 5' and 3'UTRs for hnRNP-C hits, through RBPmap, has identified that also the mouse Myc mRNA is an hnRNP-C target through the 5'UTR. Interestingly, cSetdb1 loss-of-function induced an increased abundance of cMyc mRNA (RNA-seq). In a global context of translation decrease in cSetdb1 loss-of-function condition, the translation of c-Myc should be sustained and the binding of hnRNP-C in complex with Trim71 should provide an attractive molecular mechanism. These data suggest that cSetdb1 regulates c-Myc expression at mRNA level and, at protein level, potentially by acting on Trim71 complex integrity, increasing the recruitment of hnRNP-C on c-Myc mRNA, through Trim71. C-Myc is a known transcription factor, required for ESC self-renewal, maintenance of mESCs identity and iPSC reprogramming. Since c-Myc overexpression can activate apoptotic cell death,[43,44] it is tempting to propose that c-Myc overexpression under cSetdb1 loss-of-function could contribute, together with the decrease in the amount of newly synthesized proteins, to the main observed phenotype of ES cell death observed under cSetdb1 loss-of-function.

Our data suggest that in the absence of cytoplasmic Setdb1, the enhanced interaction between Trim71 and hnRNP-c promotes translation of Trim71 target mRNAs such as *c-myc* (Figure S8). Conversely, cytoplasmic Setdb1 interacts with Trim71 and possibly recruits DCP1a, since we have shown by PLA a close proximity between DCP1a and Trim71, and also between DCP1 and Setdb1 (Figures 2D and S4C, Video S2), stabilizing a transient Trim71-Setdb1-DCP1a complex and leading to translation decrease and mRNA degradation.

In conclusion, we showed that cytoplasmic Setdb1 has an essential function, independent of Setdb1 nuclear role, key for ESCs and the regulation of their fate. This essential function is exerted at a post-transcriptional level of gene expression regulation, and it can be, at least in part, explained by the interaction with the ESC-specific mRNA silencer Trim71 and the crucial role of Setdb1 for the integrity of Trim71 complex. Our data unravel a new role of Setdb1 in post-transcriptional regulation of gene expression and suggest that the cytoplasmic dysregulations, caused by the loss of cSetdb1 functions, affect ES identity and survival.

Limitations of the study

To explore the role of cSetdb1 in post-transcriptional regulation of gene expression, we focused on the E3 ubiquitin ligase and mRNA silencer Trim71/Lin41. Since Trim71 is not widely expressed but its expression is restricted to stem cells, consequently, the role of cSETDB1 through the regulation of Trim71 complex integrity would be limited to this context.

STAR★METHODS

Detailed methods are provided in the online version of this paper and include the following:

- KEY RESOURCES TABLE
- RESOURCE AVAILABILITY
  - Lead contact
  - Materials availability
  - Data and code availability
- EXPERIMENTAL MODEL AND SUBJECT DETAILS
  - Cell lines and cell culture
- METHOD DETAILS
  - Cloning and generation of the Setdb1-NLS stable cell line
  - Transfection
  - Cell count
  - ChIP-qPCR
  - RNA purification and quantitative reverse transcription-PCR (RT-qPCR)
  - RNA-seq
  - Annexin V assay
  - SUnSET assay
  - Immunofluorescence (IF) and imaging
  - DuoLink
  - Total protein extracts
  - *In vitro* methylation assay
  - Cell fractionation, co-immunoprecipitation and mass spectrometry sample preparation
  - Western blot
  - Yeast-2-Hybrid screen
  - Antibodies
- QUANTIFICATION AND STATISTICAL ANALYSIS
  - Bioinformatic analyses of RNA-seq data
  - Mass spectrometry data analyses
  - Statistical analyses

SUPPLEMENTAL INFORMATION

Supplemental information can be found online at https://doi.org/10.1016/j.isci.2023.107386.

AUTHOR CONTRIBUTIONS

Conceptualization, S.A.S. and B.C.; Methodology, R.P., L.D.M., C.B., V.J., B.C., and S.A.S.; Software, C.B.; Formal Analysis, B.C. and C.B.; Investigation, R.P., L.D.M., C.B., S.A., P.C.T, V.J., and B.C.; Data Curation, B.C. and C.B.; Writing – Original draft, R.P., B.C., and S.A.S.; Writing – Review and Editing, R.P., L.D.M., C.B., V.J., B.C., and S.A.S.; Visualization, R.P., L.D.M., C.B., V.J., B.C., and S.A.S.; Supervision, B.C. and S.A.S.; Funding Acquisition, S.A.S; Project Administration, B.C. and S.A.S.

REFERENCES

1. Gabut, M., Bourdelais, F., and Durand, S. (2020). Ribosome and Translational Control in Stem Cells. Cells 9. https://doi.org/10.3390/cells9020497.

2. Kwon, S.C., Yi, H., Eichelbaum, K., Föhr, S., Fischer, B., You, K.T., Castello, A., Krijgsveld, J., Hentze, M.W., and Kim, V.N. (2013). The RNA-binding protein repertoire of embryonic stem cells. Nat. Struct. Mol. Biol. 20, 1122–1130. https://doi.org/10.1038/nsmb.2638.

3. Ye, J., and Blelloch, R. (2014). Regulation of pluripotency by RNA binding proteins. Cell Stem Cell 15, 271–280. https://doi.org/10.1016/j.stem.2014.08.010.

4. You, K.T., Park, J., and Kim, V.N. (2015). Role of the small subunit processome in the maintenance of pluripotent stem cells. Genes Dev. 29, 2004–2009. https://doi.org/10.1101/gad.267112.115.

5. Dodge, J.E., Kang, Y.K., Beppu, H., Lei, H., and Li, E. (2004). Histone H3-K9 methyltransferase ESET is essential for early development. Mol. Cell Biol. 24, 2478–2486.

6. Bilodeau, S., Kagey, M.H., Frampton, G.M., Rahl, P.B., and Young, R.A. (2009). SetDB1 contributes to repression of genes encoding developmental regulators and maintenance of ES cell state. Genes Dev. 23, 2484–2489. 23/21/2484 [pii]. https://doi.org/10.1101/gad.1837309.

7. Lohmann, F., Loureiro, J., Su, H., Fang, Q., Lei, H., Lewis, T., Yang, Y., Labow, M., Li, E., Chen, T., and Kadam, S. (2010). KMT1E mediated H3K9 methylation is required for the maintenance of embryonic stem cells by repressing trophectoderm differentiation. Stem Cell. 28, 201–212. https://doi.org/10.1002/stem.278.

8. Yeap, L.S., Hayashi, K., and Surani, M.A. (2009). ERG-associated protein with SET domain (ESET)-Oct4 interaction regulates pluripotency and represses the trophectoderm lineage. Epigenet. Chromatin 2, 12. 1756-8935-2-12 [pii]. https://doi.org/10.1186/1756-8935-2-12.

9. An, J., Zhang, X., Qin, J., Wan, Y., Hu, Y., Liu, T., Li, J., Dong, W., Du, E., Pan, C., and Zeng, W. (2014). The histone methyltransferase ESET is required for the survival of spermatogonial stem/progenitor cells in mice. Cell Death Dis. 5, e1196. cddis2014171 [pii]. https://doi.org/10.1038/cddis.2014.171.

10. Lawson, K.A., Teteak, C.J., Zou, J., Hacquebord, J., Ghatan, A., Zielinska-Kwiatkowska, A., Fernandes, R.J., Chansky, H.A., and Yang, L. (2013). Mesenchyme-specific knockout of ESET histone methyltransferase causes ectopic hypertrophy and terminal differentiation of articular chondrocytes. J. Biol. Chem. 288, 32119–32125. M113.473827 [pii]. https://doi.org/10.1074/jbc.M113.473827.

11. Tan, S.L., Nishi, M., Ohtsuka, T., Matsui, T., Takemoto, K., Kamio-Miura, A., Aburatani, H., Shinkai, Y., and Kageyama, R. (2012). Essential roles of the histone methyltransferase ESET in the epigenetic control of neural progenitor cells during development. Development 139, 3806–3816. 139/20/3806 [pii]. https://doi.org/10.1242/dev.082198.

12. Lawson, K.A., Teteak, C.J., Gao, J., Li, N., Hacquebord, J., Ghatan, A., Zielinska-Kwiatkowska, A., Song, G., Chansky, H.A., and Yang, L. (2013). ESET histone methyltransferase regulates osteoblastic differentiation of mesenchymal stem cells during postnatal bone development. FEBS Lett. 587, 3961–3967. S0014-5793(13)00798-9 [pii]. https://doi.org/10.1016/j.febslet.2013.10.028.

13. Beyer, S., Pontis, J., Schirwis, E., Battisti, V., Rudolf, A., Le Grand, F., and Ait-Si-Ali, S. (2016). Canonical Wnt signalling regulates nuclear export of Setdb1 during skeletal muscle terminal differentiation. Cell Discov. 2, 16037. https://doi.org/10.1038/celldisc.2016.37.

14. Yang, L., Lawson, K.A., Teteak, C.J., Zou, J., Hacquebord, J., Patterson, D., Ghatan, A.C., Mei, Q., Zielinska-Kwiatkowska, A., Bain, S.D., et al. (2013). ESET histone methyltransferase is essential to hypertrophic differentiation of growth plate chondrocytes and formation of epiphyseal plates. Dev. Biol. 380, 99–110. S0012-1606(13)00225-X [pii]. https://doi.org/10.1016/j.ydbio.2013.04.031.

15. Loyola, A., Bonaldi, T., Roche, D., Imhof, A., and Almouzni, G. (2006). PTMs on H3 variants before chromatin assembly potentiate their final epigenetic state. Mol. Cell. 24, 309–316. S1097-2765(06)00600-9 [pii]. https://doi.org/10.1016/j.molcel.2006.08.019.

16. Schultz, D.C., Ayyanathan, K., Negorev, D., Maul, G.G., and Rauscher, F.J., 3rd (2002). SETDB1: a novel KAP-1-associated histone H3, lysine 9-specific methyltransferase that contributes to HP1-mediated silencing of euchromatic genes by KRAB zinc-finger proteins. Genes Dev. 16, 919–932. https://doi.org/10.1101/gad.973302.

17. Lin, Y., Zhang, F., Chen, S., Zhu, X., Jiao, J., Zhang, Y., Li, Z., Lin, J., Ma, B., Chen, M., et al. (2023). Binary Colloidal Crystals Promote Cardiac Differentiation of Human Pluripotent Stem Cells via Nuclear Accumulation of SETDB1. ACS Nano 17, 3181–3193. https://doi.org/10.1021/acsnano.3c00009.

18. Cho, S., Park, J.S., and Kang, Y.K. (2013). Regulated nuclear entry of over-expressed Setdb1. Gene Cell. 18, 694–703. https://doi.org/10.1111/gtc.12068.

19. Matsui, T., Leung, D., Miyashita, H., Maksakova, I.A., Miyachi, H., Kimura, H., Tachibana, M., Lorincz, M.C., and Shinkai, Y. (2010). Proviral silencing in embryonic stem cells requires the histone methyltransferase ESET. Nature 464, 927–931. https://doi.org/10.1038/nature08858.

20. Fisher, C.L., Marks, H., Cho, L.T.Y., Andrews, R., Wormald, S., Carroll, T., Iyer, V., Tate, P., Rosen, B., Stunnenberg, H.G., et al. (2017). An efficient method for generation of bi-allelic null mutant mouse embryonic stem cells and its application for investigating epigenetic modifiers. Nucleic Acids Res. 45, e174. https://doi.org/10.1093/nar/gkx811.

21. Thompson, P.J., Dulberg, V., Moon, K.M., Foster, L.J., Chen, C., Karimi, M.M., and Lorincz, M.C. (2015). hnRNP K coordinates transcriptional silencing by SETDB1 in embryonic stem cells. PLoS Genet. 11, e1004933. https://doi.org/10.1371/journal.pgen.1004933.

22. Chang, H.M., Martinez, N.J., Thornton, J.E., Hagan, J.P., Nguyen, K.D., and Gregory, R.I. (2012). Trim71 cooperates with microRNAs to repress Cdkn1a expression and promote embryonic stem cell proliferation. Nat. Commun. 3, 923. https://doi.org/10.1038/ncomms1909.

23. Loedige, I., Gaidatzis, D., Sack, R., Meister, G., and Filipowicz, W. (2013). The mammalian TRIM-NHL protein TRIM71/LIN-41 is a repressor of mRNA function. Nucleic Acids Res. 41, 518–532. https://doi.org/10.1093/nar/gks1032.

24. Torres-Fernández, L.A., Jux, B., Bille, M., Port, Y., Schneider, K., Geyer, M., Mayer, G., and

Kolanus, W. (2019). The mRNA repressor TRIM71 cooperates with Nonsense-Mediated Decay factors to destabilize the mRNA of CDKN1A/p21. Nucleic Acids Res. 47, 11861–11879. https://doi.org/10.1093/nar/gkz1057.

25. Schwanhäusser, B., Busse, D., Li, N., Dittmar, G., Schuchhardt, J., Wolf, J., Chen, W., and Selbach, M. (2011). Global quantification of mammalian gene expression control. Nature 473, 337–342. https://doi.org/10.1038/nature10098.

26. Wu, K., Liu, H., Wang, Y., He, J., Xu, S., Chen, Y., Kuang, J., Liu, J., Guo, L., Li, D., et al. (2020). SETDB1-Mediated Cell Fate Transition between 2C-Like and Pluripotent States. Cell Rep. 30, 25–36.e6. https://doi.org/10.1016/j.celrep.2019.12.010.

27. Welte, T., Tuck, A.C., Papasaikas, P., Carl, S.H., Flemr, M., Knuckles, P., Rankova, A., Bühler, M., and Großhans, H. (2019). The RNA hairpin binder TRIM71 modulates alternative splicing by repressing MBNL1. Genes Dev. 33, 1221–1235. https://doi.org/10.1101/gad.328492.119.

28. Van Nostrand, E.L., Pratt, G.A., Shishkin, A.A., Gelboin-Burkhart, C., Fang, M.Y., Sundararaman, B., Blue, S.M., Nguyen, T.B., Surka, C., Elkins, K., et al. (2016). Robust transcriptome-wide discovery of RNA-binding protein binding sites with enhanced CLIP (eCLIP). Nat. Methods 13, 508–514. https://doi.org/10.1038/nmeth.3810.

29. Kim, J.H., Paek, K.Y., Choi, K., Kim, T.D., Hahm, B., Kim, K.T., and Jang, S.K. (2003). Heterogeneous nuclear ribonucleoprotein C modulates translation of c-myc mRNA in a cell cycle phase-dependent manner. Mol. Cell Biol. 23, 708–720. https://doi.org/10.1128/mcb.23.2.708-720.2003.

30. Mitschka, S., Ulas, T., Goller, T., Schneider, K., Egert, A., Mertens, J., Brüstle, O., Schorle, H., Beyer, M., Klee, K., et al. (2015). Co-existence of intact stemness and priming of neural differentiation programs in mES cells lacking Trim71. Sci. Rep. 5, 11126. https://doi.org/10.1038/srep11126.

31. Rivera, C., Saavedra, F., Alvarez, F., Díaz-Celis, C., Ugalde, V., Li, J., Forné, I., Gurard-Levin, Z.A., Almouzni, G., Imhof, A., and Loyola, A. (2015). Methylation of histone H3 lysine 9 occurs during translation. Nucleic Acids Res. 43, 9097–9106. https://doi.org/10.1093/nar/gkv929.

32. Schmidt, E.K., Clavarino, G., Ceppi, M., and Pierre, P. (2009). SUnSET, a nonradioactive method to monitor protein synthesis. Nat. Methods 6, 275–277. https://doi.org/10.1038/nmeth.1314.

33. Sampath, P., Pritchard, D.K., Pabon, L., Reinecke, H., Schwartz, S.M., Morris, D.R., and Murry, C.E. (2008). A hierarchical network controls protein translation during murine embryonic stem cell self-renewal and differentiation. Cell Stem Cell 2, 448–460. https://doi.org/10.1016/j.stem.2008.03.013.

34. Takai, H., Masuda, K., Sato, T., Sakaguchi, Y., Suzuki, T., Suzuki, T., Koyama-Nasu, R., Nasu-Nishimura, Y., Katou, Y., Ogawa, H., et al. (2014). 5-Hydroxymethylcytosine plays a critical role in glioblastomagenesis by recruiting the CHTOP-methylosome complex. Cell Rep. 9, 48–60. https://doi.org/10.1016/j.celrep.2014.08.071.

35. Chang, C.T., Hautbergue, G.M., Walsh, M.J., Viphakone, N., van Dijk, T.B., Philipsen, S., and Wilson, S.A. (2013). Chtop is a component of the dynamic TREX mRNA export complex. EMBO J. 32, 473–486. https://doi.org/10.1038/emboj.2012.342.

36. Yang, X., Yang, Y., Sun, B.F., Chen, Y.S., Xu, J.W., Lai, W.Y., Li, A., Wang, X., Bhattarai, D.P., Xiao, W., et al. (2017). 5-methylcytosine promotes mRNA export - NSUN2 as the methyltransferase and ALYREF as an m(5)C reader. Cell Res. 27, 606–625. https://doi.org/10.1038/cr.2017.55.

37. Jeffery, L., and Nakielny, S. (2004). Components of the DNA methylation system of chromatin control are RNA-binding proteins. J. Biol. Chem. 279, 49479–49487. https://doi.org/10.1074/jbc.M409070200.

38. Aeschimann, F., Kumari, P., Bartake, H., Gaidatzis, D., Xu, L., Ciosk, R., and Großhans, H. (2017). LIN41 Post-transcriptionally Silences mRNAs by Two Distinct and Position-Dependent Mechanisms. Mol. Cell. 65, 476–489.e4. https://doi.org/10.1016/j.molcel.2016.12.010.

39. Rybak, A., Fuchs, H., Hadian, K., Smirnova, L., Wulczyn, E.A., Michel, G., Nitsch, R., Krappmann, D., and Wulczyn, F.G. (2009). The let-7 target gene mouse lin-41 is a stem cell specific E3 ubiquitin ligase for the miRNA pathway protein Ago2. Nat. Cell Biol. 11, 1411–1420. https://doi.org/10.1038/ncb1987.

40. Worringer, K.A., Rand, T.A., Hayashi, Y., Sami, S., Takahashi, K., Tanabe, K., Narita, M., Srivastava, D., and Yamanaka, S. (2014). The let-7/LIN-41 pathway regulates reprogramming to human induced pluripotent stem cells by controlling expression of prodifferentiation genes. Cell Stem Cell 14, 40–52. https://doi.org/10.1016/j.stem.2013.11.001.

41. Castello, A., Fischer, B., Eichelbaum, K., Horos, R., Beckmann, B.M., Strein, C., Davey, N.E., Humphreys, D.T., Preiss, T., Steinmetz, L.M., et al. (2012). Insights into RNA biology from an atlas of mammalian mRNA-binding proteins. Cell 149, 1393–1406. https://doi.org/10.1016/j.cell.2012.04.031.

42. Christian, K.J., Lang, M.A., and Raffalli-Mathieu, F. (2008). Interaction of heterogeneous nuclear ribonucleoprotein C1/C2 with a novel cis-regulatory element within p53 mRNA as a response to cytostatic drug treatment. Mol. Pharmacol. 73, 1558–1567. https://doi.org/10.1124/mol.107.042507.

43. Prendergast, G.C. (1999). Mechanisms of apoptosis by c-Myc. Oncogene 18, 2967–2987. https://doi.org/10.1038/sj.onc.1202727.

44. McMahon, S.B. (2014). MYC and the control of apoptosis. Cold Spring Harb. Perspect. Med. 4, a014407. https://doi.org/10.1101/cshperspect.a014407.

45. Zakharova, V.V., Magnitov, M.D., Del Maestro, L., Ulianov, S.V., Glentis, A., Uyanik, B., Williart, A., Karpukhina, A., Demidov, O., Joliot, V., et al. (2022). SETDB1 fuels the lung cancer phenotype by modulating epigenome, 3D genome organization and chromatin mechanical properties. Nucleic Acids Res. 50, 4389–4413. https://doi.org/10.1093/nar/gkac234.

46. Fritsch, L., Robin, P., Mathieu, J.R.R., Souidi, M., Hinaux, H., Rougeulle, C., Harel-Bellan, A., Ameyar-Zazoua, M., and Ait-Si-Ali, S. (2010). A subset of the histone H3 lysine 9 methyltransferases Suv39h1, G9a, GLP, and SETDB1 participate in a multimeric complex. Mol. Cell. 37, 46–56. S1097-2765(09)00921-6 [pii]. https://doi.org/10.1016/j.molcel.2009.12.017.

47. Vojtek, A.B., Hollenberg, S.M., and Cooper, J.A. (1993). Mammalian Ras interacts directly with the serine/threonine kinase Raf. Cell 74, 205–214. https://doi.org/10.1016/0092-8674(93)90307-c.

48. Cunningham, F., Achuthan, P., Akanni, W., Allen, J., Amode, M.R., Armean, I.M., Bennett, R., Bhai, J., Billis, K., Boddu, S., et al. (2019). Ensembl 2019. Nucleic Acids Res. 47, D745–D751. https://doi.org/10.1093/nar/gky1113.

49. Dobin, A., Davis, C.A., Schlesinger, F., Drenkow, J., Zaleski, C., Jha, S., Batut, P., Chaisson, M., and Gingeras, T.R. (2013). STAR: ultrafast universal RNA-seq aligner. Bioinformatics 29, 15–21. https://doi.org/10.1093/bioinformatics/bts635.

50. Liao, Y., Smyth, G.K., and Shi, W. (2019). The R package Rsubread is easier, faster, cheaper and better for alignment and quantification of RNA sequencing reads. Nucleic Acids Res. 47, e47. https://doi.org/10.1093/nar/gkz114.

51. Yu, G., Wang, L.G., Han, Y., and He, Q.Y. (2012). clusterProfiler: an R package for comparing biological themes among gene clusters. OMICS 16, 284–287. https://doi.org/10.1089/omi.2011.0118.

52. Yates, A.D., Achuthan, P., Akanni, W., Allen, J., Allen, J., Alvarez-Jarreta, J., Amode, M.R., Armean, I.M., Azov, A.G., Bennett, R., et al. (2020). Ensembl 2020. Nucleic Acids Res. 48, D682–D688. https://doi.org/10.1093/nar/gkz966.

53. Paz, I., Kosti, I., Ares, M., Jr., Cline, M., and Mandel-Gutfreund, Y. (2014). RBPmap: a web server for mapping binding sites of RNA-binding proteins. Nucleic Acids Res. 42, W361–W367. https://doi.org/10.1093/nar/gku406.

STAR★METHODS

KEY RESOURCES TABLE

REAGENT or RESOURCE	SOURCE	IDENTIFIER
Antibodies		
Setdb1	Abcam	ab107225
Vinculin	Sigma	V9131
alpha-tubulin	Sigma	T9026
GLP	R&D	B0422-00
Trim71	Fitzerald	70R-11-707
GFP	Santa Cruz	sc-9996
GM130	BD	610822
eEF1A	Abcam	ab37969
Rpl5	GeneTex	GTX101821
beta-actin	Sigma	A5441
GAPDH	Sigma	G9545
eIF3c	Novusbio	NB100-500
SDHA	CST	11998
Ago2	Abcam	ab32381
c-myc	Sigma	Clone 7E18
Myc-Trap	ChromoteK	yta-20
GFP-trap	ChromoteK	gta-20
Puromycin	Millipore	MABE343
Chemicals, peptides, and recombinant proteins		
Recombinant histone H3.1	NEB	M2503S
Critical commercial assays		
FITC Annexin V Apoptosis Detection Kit	BD Biosciences	RRID: AB_2869082
Duolink™ *In Situ* kit	Sigma	DUO92101
Deposited data		
mESCs RNAseq of Setdb1 knock-out and reexpression of a WT, a catalytic-dead variant (CA) or a NLS-tagged Setdb1 protein	https://zenodo.org/record/6791943#.YsMqM4TP0uU	https://doi.org/10.5281/zenodo 6791943
mESCs proteomic of Trim71 partners after Setdb1 acute depletion	https://zenodo.org/record/6795454#.YsMnnYTP0uV	https://doi.org/10.5281/zenodo.6795454
Experimental models: Cell lines		
Setdb1 conditional knockout (cKO) mESCs	Pr Yoichi Shinkai	Matsui et al.[19]
Oligonucleotides		
oligonucleotides	See Table S7	Table S7
Recombinant DNA		
pCAG-3XFLAG-IRESbsd plasmid	Pr Yoichi Shinkai	pCAG-3XFLAG-IRESbsd
pCMV-2N-3T plasmid	Dr Tony Kouzarides	pCMV-2N-3T
Myc-pCS2 plasmid	Dr Liu Yang	Myc-pCS2
3xFLAG-WT-Setdb1 plasmid	This study	3xFLAG-WT-Setdb1
3xFLAG-CA-Setdb1 plasmid	This study	3xFLAG-CA-Setdb1
3xFLAG-NLS-Setdb1 plasmid	This study	3xFLAG-CA-Setdb1

Continued

REAGENT or RESOURCE	SOURCE	IDENTIFIER
Trim71-pCS2 plasmid	This study	Trim71-pCS2
GFP-Trim71 plasmid	This study	GFP-Trim71
Software and algorithms		
Repository for the downstream analysis of the Setdb1 KO, CA, AA and NLS experiments.	This paper	https://github.com/parisepigenetics/setdb1-downstream-anal

RESOURCE AVAILABILITY

Lead contact

Further information and requests for resources and reagents should be directed to and will be fulfilled by the lead contact, Slimane Ait-Si-Ali (slimane.aitsiali@u-paris.fr).

Materials availability

This study did not generate new unique reagents. All reagents generated in this study are available from the lead contact with a completed Materials Transfer Agreement.

Data and code availability

All original code has been deposited at Github [https://github.com/parisepigenetics/setdb1-downstream-anal] and is publicly available as of the date of publication. It has been listed in the key resources table.

All original data has been deposited at Zenodo and is publicly available as of the date of publication. DOIs are listed in the key resources table.

EXPERIMENTAL MODEL AND SUBJECT DETAILS

Cell lines and cell culture

Setdb1 conditional knockout (cKO) mESCs are a generous gift form Pr Yoichi Shinkai (Matsui et al., 2010). Yoichi Shinkai's group genetically modified mESCs TT2 cells to create *Setdb1* cKO and KO alleles. The Setdb1 cKO allele contains a 3′ truncated exon 15 and a stop codon inserted in front of this exon. To generate the *Setdb1* cKO allele, exons 15 and 16, which encode the core amino acids of the catalytic domain, have been flanked with two lox-P sites recognized by Cre recombinase enzyme. Cre-estrogen receptor fusion gene Mer-Cre-Mer has been introduced to induce acute Setdb1 KO after Tamoxifen treatment. Setdb1 cKO mESCs where Setdb1 expression is stably rescued by wild type 3xFlag-Setdb1 (WT) or by the catalytic dead mutant 3xFlag-Setdb1 (CA) were generously given by Pr Yoichi Shinkai. The catalytic dead mutant was obtained with a single lysine mutation. In the lab, Setdb1 cKO mESCs, where Setdb1 expression is stably rescued by NLS-3xFlag-Setdb1 which localizes only in the nucleus, have been established (2 NLS sequences have been added in order to retain Setdb1 in the nucleus, detailed in the next chapter). All mESCs were cultured in Dulbecco's modified Eagle's Medium DMEM (Sigma) supplemented with 15% fetal calf serum (Gibco), 1% penicillin/streptomycin (Sigma), 0.1 mM β-mercaptoethanol (Thermo), 1 mM non-essential amino acids (Sigma), and 1000 U/mL of Leukemia Inhibitory Factor (LIF) (Millipore). All mESC lines were cultured in standard feeder-free conditions with 0.2% gelatin, maintained at 37°C and 8% CO_2. To induce deletion of the Setdb1 cKO allele, mESCs were cultured in 800 nM 4-Hydroxy Tamoxifen (Sigma).

METHOD DETAILS

Cloning and generation of the Setdb1-NLS stable cell line

Setdb1 cDNA in frame with cDNA encoding for 2 copies of the widely used NLS sequence APKKKRKVAD, were cloned into pCAG-3XFLAG-IRESbsd vector used by Pr Yoichi Shinkai lab to express 3xFLAG-WT Setdb1 and 3xFLAG-CA Setdb1. The NLS sequences were derived from the pCMV-2N-3T vector (a kind gift of Dr Tony Kouzarides), which contains two nuclear localization signals and three HA-epitope tags. The pCMV-2N-3T vector has been extensively used to ensure nuclear localization of nuclear protein deletion mutants in which the original NLS is deleted. Clones were selected in medium containing Blasticidin

(7 mg/mL). Full-length Trim71 cDNA was cloned into pCS2 vector given by Liu Yang, which contains a Myc epitope tag.

Transfection

Plasmids were transiently transfected into mESCs using lipofectamine 2000 (Life Technologies). After transfection of plasmids expressing Myc-Trim71 or GFP-Trim71, cells were harvested at 24h post-transfection for immunoprecipitation, immunofluorescence, PLA assay and western blot analysis. For ChIP-qPCR experiments (see below), cells were transfected at day 0 and day 2 with a plasmid expressing 3xFLAG-WT Setdb1 and 3xFLAG-NLS Setdb1 described above and harvested at day 3.

Cell count

Harvested cells were resuspended in media or PBS in 0.2% Trypan Blue. Live cells were counted using countess automated Cell Counter (Invitrogen) according to the manufacturer instructions.

ChIP-qPCR

Cell extracts were processed for ChIP-qPCR experiments (native ChIP) as in[45]. H3K9m3 values for KO and KO+NLS cells were expressed as a percentage of respectively the level in Ctr cells and KO+WT cells. The value for KO+NLS cells was normalized using the ratio of exogenous Setdb1 protein level between KO+NLS and KO+WT cells determined by Western blot quantification.

RNA purification and quantitative reverse transcription-PCR (RT-qPCR)

Total RNAs were extracted using RNeasy mini-kit (Qiagen) following manufacturer's procedures. DNase (Qiagen) treatment was performed to remove residual DNA. With High-Capacity cDNA Reverse Transcription Kit (Applied Biosystems), 1 μg of total RNAs was reverse-transcribed (RT). Real-time quantitative PCR was performed to analyze relative gene expression levels using SYBR Green Master mix (Promega) following manufacturer indications. Relative expression values were normalized to the housekeeping *Gapdh* mRNA. RNA- and RT- were used as negative controls. Oligonucleotide list is provided in Table S7.

RNA-seq

RNA was isolated as described above (RNA purification section). After RNA extraction, the amount of RNAs was quantified by Nanodrop. The quality of the RNA was determined on the Agilent 2100 Bioanalyzer (Agilent Technologies, Palo Alto, CA, USA), the RNA integrity number was above 8 for all the samples. To construct libraries, 1 mg of high-quality total RNA sample was processed using Truseq® stranded total RNA kit (Illumina®). After the removal of ribosomal RNAs (using Ribo-zero® rRNA), confirmed by QC control on pico chipTM on the Agilent 2100 Bioanalyzer (Agilent Technologies, Palo Alto, CA, USA), total RNA molecules are fragmented and reverse-transcribed using random primers. Replacement of dTTP by dUTP during the second strand synthesis will permit to achieve the strand specificity. Addition of a single A base to the cDNA is followed by ligation of adapters. Libraries were quantified by qPCR using the KAPA Library Quantification Kit for Illumina Libraries (KapaBiosystems) and library profiles were assessed using the DNA High SensitivityTMHS kit on an Agilent Bioanalyzer 2100. Libraries were sequenced on an Illumina® Next-seq 500 instrument using 75 base-lengths read V2 chemistry in a paired-end mode.

Annexin V assay

Cells were trypsinized and resuspended in 1X Binding Buffer. 10^5 cells were incubated for 15 min at RT under lightless condition in 1X Annexin V binding buffer containing FITC Annexin V and propidium iodide according to FITC Annexin V Apoptosis Detection Kit (BD Biosciences). 10.000 cells were sampled on BD FACSCaliburTM flow cytometer and cells were gated based on forward and side scatter. Fluorescence measurements were detected on the FL1 (Annexin V) and FL2 (PI). Data were analyzed using FlowJo software.

SUnSET assay

mESCs were treated with Puromycin for 20min at 37°C then washed with medium for 20 min at 37°C. After trypsinization and washes in PBS the cells were fixed with 2% formaldehyde (Electron Microscopy Sciences) for 15 min, quench with 50 mM NH4Cl for 10 min and permeabilized with 0.2% Triton X-100 for 5 min. Primary antibody against puromycin and Alexa-488 fluorescent secondary antibody were diluted in NH4Cl containing 10% SVF serum and incubated with cells for 1 hour each at room temperature. The cells were

washed and resuspended in PBS. 10.000 cells were sampled on BD FACSCaliburTM flow cytometer and cells were gated based on forward and side scatter. Fluorescence measurements were detected on the FL1. Data were analyzed using FlowJo software.

Immunofluorescence (IF) and imaging

Cells were grown on glass coverslips coated with laminin 10 mg/ml in PBS for 1 h at 37°C. mESCs cells were fixed with 4% formaldehyde (Electron Microscopy Sciences) for 20 min, quench with 50 mM NH4Cl for 10 min and permeabilized with 0.5% Triton-X-100 for 5 min. Primary and secondary antibodies were diluted in PBS containing 2% SVF serum and 0.1% Tween and incubated with coverslips overnight at 4°C or 1h at room temperature, respectively. DNA was stained with 1 μg ml−1 DAPI (Life Technology). Coverslips were mounted with Vectashield mounting media (Vector labs). Microscopy was performed using inverted microscope Leica DMI- 6000. Images were taken with the HQ2 Coolsnap motorized by Metamorph software. All images were processed with ImageJ software.

DuoLink

Cells were prepared and fixed as described above (IF section). Primary and secondary antibodies were incubated according to manufacturer procedure from Duolink™ *In Situ* kit (Sigma DUO92101). The addition of Minus and Plus probes, the ligation and the amplification steps were carried out following manufacturer indications. Coverslips were stained with DAPI and mounted following manufacturer indications. Microscopy was performed using inverted microscope Leica DMI- 6000. Images were taken with the HQ2 Coolsnap motorized by Metamorph software. All images were processed with ImageJ software.

Total protein extracts

Cells were lysed in RIPA buffer to which protease and phosphatase inhibitors (Sigma) were added. After 30 min of incubation, sonication was performed for 10 min (30 sec ON, 30 sec OFF) at medium frequency (Bioruptor, Diagenode). The lysate was centrifugate at 16.103 RCF for 10 min. Proteins were quantified using Pierce™ BCA™kit.

In vitro methylation assay

In vitro methylation assays were performed using normalized amount of flag immunoprecipitated (with the beads) SETDB1 (WT or CA or NLS) from total extract of stable ES cell lines, 1 μg recombinant H3.1 (NEB M2503S and 2 μl Adenosyl-L-methionine, S-[methyl-3H] (Perkin Elmer NET155V250C) in 50mM Tris pH8,20 mM KCl, 5 mM MgCl2, 1 mM DTT, 5% glycerol and incubated at 30°C for 2 hours. Samples were separated on 4-12% NUPAGE gels (Invitrogen NP0321BOX) in MOPS buffer (Invitrogen NP0001), Coomassie stained (Invitrogen LC6060). Then gel was dried and autoradiography performed on Amersham Hyperfilm (ref28906843) at -80°C.

Cell fractionation, co-immunoprecipitation and mass spectrometry sample preparation

Cells were lysed in buffer A (20 mM HEPES pH 7, 0.15 mM EDTA, 0.15 mM EGTA, 10 mM KCl), 10% NP40 and SR buffer (50 mM HEPES pH 7, 0.25 mM EDTA, 10 mM KCl, 70% (m/v) sucrose) with the addition of protease and phosphatase inhibitors (Sigma). Cell lysates were centrifuged at 2000 g for 5 min and the supernatant was recovered (cytoplasmic fraction) (as in[46]). Then high and low salt buffer were added (20 mM Tris-HCl pH 7.65; 0.2 mM EDTA; 25% glycerol; 900 mM NaCl; 1.5 mM MgCl2) to a final NaCl concentration of 300 mM to extract nuclear proteins. The nuclear extracts were next treated with Micrococcal nuclease (0.0125 U/ml) at 37°C during 10 min in addition to 1 mM CaCl2. EDTA was then added to 4 mM final concentration in order to stop the nuclease reaction. Finally, sonication was performed for 10 min (30 sec ON, 30 sec OFF) at medium frequency (Bioruptor Diagenode). The nuclear and cytoplasmic fractions were ultra-centrifuged at 40000 rpm for 30 min and pre-cleared with protein G-agarose beads (Sigma) during 2h at 4°C. Immunoprecipitations were carried out overnight at 4°C using 5 μg of each antibody. Ultralink A/G beads (Perbio) were blocked overnight at 4°C with 0.3 % BSA and 0.5 μg/μl ssDNA and then incubated with the immunocomplexes the next day for 2 h, at 4°C.

For immunoprecipitation using Myc-Trap technology, the Myc-Trap beads were equilibrated with wash buffer (10 mM Tris pH 7.5, 150 mM NaCl, 0.15 mM EDTA). Immunoprecipitations were carried out for 1 h or overnight at 4°C using 25 μL of Myc-Trap bead slurry. The immunocomplexes were washed four times in wash buffer and the proteins were eluted in NuPAGE 4X loading buffer (Life Technologies) and

10X reducing agent at 96°C during 5 min. Finally, the samples were examined either by western blot or by mass spectrometry at the Taplin facility (as in[46]).

Western blot

Total, nuclear or cytoplasmic protein extracts, or IP samples were prepared in NuPAGE 4X loading buffer (Life Technologies) and 10X reducing agent and hit at 96°C for 5 min. Separations of proteins were performed using pre-cast polyacrylamide gel cassettes (NuPAGE® Novex® 4-12% Bis-Tris) (Life technologies) and 1X NuPAGE MOPS SDS Running Buffer and transferred into nitrocellulose membranes in 20 mM phosphate transfer buffer (pH 6.7). Membranes were blocked in PBS supplemented with 0.1% Tween 20 and 5% non-fat dried milk and incubated with primary antibodies. Primary antibodies were detected with IRDYE- conjugated secondary antibodies and scanned on the LI-COR imaging system. Quantification of bands was performed with LI-COR software.

Yeast-2-Hybrid screen

Yeast-two-hybrid (Y2H) screen was performed by Hybrigenics services (as in[47]) by ULTImate Y2H screen. We used the LexA Y2H system,[47] that uses Trp1 and Leu2 as plasmid markers for the DNA Binding Domain (DBD). The test of interaction uses His3 as reporter gene. Growth test on solid DO-2 medium (-Trp, -Leu, selective for the presence of both DBD) and DO-3 medium (-Trp, -Leu, -His, selective for the interaction), was performed in duplicate. In case of autoactivation of bait or prey fragments, selection medium with increasing concentrations of 3-Aminotriazole is used. We used Mus musculus Setdb1 cDNA (reference Bait Fragment Mus musculus - Setdb1 (aa 1-1308) ; hgx4711v1) as a bait against the prey library Mouse Embryonic Stem Cell library_RP1; Vector(s) pB27 (N-LexA-bait-C fusion); Processed Clones 341 (pB27_A); Analyzed Interactions 66.7 millions (pB27_A); 3AT Concentration 5.0 mM (pB27_A).

Antibodies

Antibodies used in western blot: Setdb1 (Abcam-ab107225), Vinculin (Sigma- V9131), alpha-tubulin (Sigma- T9026), GLP (R&D-PP-B0422-00), Trim71 (Fitzerald-70R-11-707), GFP (Santa Cruz-sc-9996), GM130 (BD-610822), eEF1A (Abcam-ab37969), Rpl5 (GeneTex- GTX101821), beta-actin (Sigma- A5441), GAPDH (Sigma-G9545), eIF3c (Novusbio-NB100-500), SDHA (CST-11998), Ago2 (Abcam- ab32381), c-Myc (clone 7E18, Sigma). Antibodies used for immunoprecipitation: Myc-Trap (ChromoteK-yta-20), GFP-Trap (ChromoteK-gta-20), IgG (Santa Cruz). Antibodies used for SUnSET/FACS analyses: Anti-Puromycin (Millipore-MABE343). Secondary antibodies for IF: AF488 DONKEYF(AB')2, anti-mouse IgG (H+L) (Invitrogen).

QUANTIFICATION AND STATISTICAL ANALYSIS

Bioinformatic analyses of RNA-seq data

All sequenced reads were aligned on the GRCm38.p6 version of mouse genome, obtained from ENSEMBL,[48] using the STAR RNA-seq aligner version 2.5.2b.[49] Normalized counts table and Transcripts Per Million (TPMs) were calculated using the Rsubread package version 1.24.1.[50] Quality control of samples and sequencing was validated by standard R functions for Principal Component Analysis (PCA) and hierarchical clustering.

After fitting the linear model with DESq2, differentially expressed genes (DEGs) were predicted by applying a correction for multiple testing p-value of 0.01. From the remaining list of genes two groups for downstream analysis were selected: one with log2 Fold Change (log2FC) more than one (log2FC >= 1 and log2FC <= -1) to investigate manually several key genes and a second more strict selection of log2FC more than 1.5 (log2FC >= 1.5 and log2FC <= -1.5) to use for the automated downstream enrichment and clustering analysis. All enrichment analyses including GO, Pathways and WikiGenes enrichment as well as Gene Set Enrichment Analysis (GSEA), and visualizations were performed with the R package ClusterProfiler.[51] Clustering of DEG TPMs (Transcripts Per kilobase Millions) was performed by using R base functions for hierarchical and k-means clustering using an array of distance measures and cluster numbers such that robust clusters were obtained. Gene expression correlation matrices for DGEs were calculated by the R package NetCluster and clustering and matrix visualization with the routines of the same package. 3' and 5'UTRs were retrieved for all DEGs by the BioMart service of the ENSEMBL database[52] for the mouse C57BL/6NJ strain and all the annotated 3' and 5'UTRs were retrieved. For each gene the longest (or at least >8bps) UTR was selected for the RNA-Binding Protein analysis, which was conducted by using the

human/mouse conserved motifs of previously characterized RNA-BPs, as indicated on the online tool RBPmap.[53] Venn diagram analysis were performed by the R package eulerr.

All analyses were performed in R versions 3.5 (for the DEG identification) and 4.0 for the downstream analysis by using in-house developed scripts available at https://github.com/parisepigenetics/setdb1-downstream-anal.

Mass spectrometry data analyses

Analyses were performed on triplicates except for KO-Trim71 since one sample was distant from the other samples in PCA and had a very low sum of peptide intensities (Figure S7A). This sample was removed for the analyses, consequently two samples were used for KO-Trim71. As the Trim 71 interactors are expected to bind only to the GFP-Trim column, only the peptides with 50% of valid values were filtered, and, for the consistency of the results, displaying at least 2 valid values in at least one triplicate, allowing the selection of 826 proteins. Missing values were replaced from normal distribution before scale to interval normalization. ANOVA multi-sample test was done with a FDR of 0.1, and the Post Hoc Tukey's HSD test with a FDR of 0.05.

Statistical analyses

Statistical analyses were performed using R and Python. Statistical significance was determined by the specific tests indicated in the corresponding figure legends.